

POLITECNICO DI TORINO

Master's degree

in Automotive Engineering



Master's degree thesis

Longitudinal dynamic modelling and simulation of a full electric
vehicle

Academic supervisor:

Prof. Andrea Tonoli

Company supervisor:

Ing. Fabrizio Impinna

Author:

Fabrizio Giordano

Academic year: 2018/2019

ABSTRACT

This thesis is carried out in the context of a design of an electric vehicle. The purpose of the thesis is to model and to simulate the longitudinal dynamic behavior of a full electric vehicle, in order to design the battery pack and to evaluate the vehicle's performance and range, through the standard driving cycles NEDC and WLTC.

The work is developed in the Matlab-Simulink environment, the electric vehicle is modelled as three different blocks that interact with each other: a vehicle block, a motor block and a battery block. The modelled vehicle follows the driving cycles with two different approaches, a forward approach, where the vehicle follows strictly the imposed speed profile, and a backward approach, where the model simulates the driver that tries to follow the driving cycles. The first approach is used to evaluate the energy consumption to complete a standard cycle, this value will be exploited in the backward approach to calibrate the proportional integrative controller, that simulates the driver, and to design and verify the battery pack. The backward approach has the objective to evaluate the vehicle range, performance and to gives information about battery pack parameters as temperature, current and state of charge (SoC). In this model the greatest efforts are spent in the modelling of the battery pack block, which takes in consideration a thermal model and the open circuit voltage (OCV) against depth of discharge (DoD) cell characteristic. In the specific, the thermal model evaluates the temperature of the battery pack due to the dissipating power and provide a de-rating control on the traction torque.

The full electric vehicle used to verify the model accuracy is the Renault Zoe, because several technical data are available. The vehicle's range and performance obtained through Renault Zoe simulation are in acceptable range of accuracy (about 5%). To conclude, the model is exploited to support the battery pack design and to predict the performance and the range, in the standard driving cycles, of the of the electric vehicle in development.

ACKNOWLEDGMENTS

I would like to thank my academic supervisor Andrea Tonoli for the for the precious tips that helped me to structure properly the thesis work. I would like also to thank my company supervisor Fabrizio Impinna and all the Flag members and thesis students that helped to accomplish the final project.

TABLE OF CONTENTS

Abstract.....	3
Acknowledgments	5
List of Figures.....	9
1 Introduction.....	11
1.1 Motivation and objective of the thesis	12
1.2 Thesis structure	12
2 Forward approach model	13
2.1 Introduction.....	13
2.2 The model structure	13
2.3 The mechanical model	14
2.3.1 Vehicle data	14
2.3.2 Motor power map	14
2.3.3 Speed profiles	15
2.3.4 Performance & Power request	17
2.3.5 Energy consumption	25
2.4 The electrical model.....	26
2.4.1 Cell.....	26
2.4.2 Battery pack	28
2.5 Further considerations.....	30
2.5.1 Vehicle range	30
2.5.2 Motor design.....	30
3 Backward approach model	31
3.1 Introduction.....	31
3.2 The model overview.....	31
3.3 Vehicle block	34
3.3.1 Wheel model.....	35
3.3.2 Dynamic model.....	36
3.3.3 Range	39
3.4 Speed comparison	40
3.5 Motor block.....	41
3.5.1 Motor Map.....	42
3.5.2 Controller.....	44
3.6 Battery block.....	47
3.6.1 Current	49

3.6.2	Saturation.....	49
3.6.3	Thermal model.....	49
3.6.4	Battery pack model.....	54
3.6.5	Outputs.....	58
4	Model validation.....	61
4.1	Forward approach model results.....	65
4.2	Backward model results.....	66
5	Case study.....	69
5.1	Performance and range results:.....	70
5.1.1	NEDC range.....	72
5.1.2	WLTC range.....	74
5.2	Battery parameters.....	76
5.3	Regenerative braking.....	77
5.3.1	Total range comparison.....	78
5.4	Thermal battery management.....	80
6	User guide.....	81
6.1	Matlab.....	81
6.1.1	Run.....	81
6.1.2	Vehicle.....	82
6.1.3	Motor.....	83
6.1.4	Battery.....	84
6.1.5	Thermal model.....	85
6.1.6	Workbench.....	85
6.2	Simulink.....	86
6.2.1	Speed cycles.....	87
7	Conclusion.....	89
8	Bibliography.....	91

LIST OF FIGURES

Figure 1: Forward approach model structure.	13
Figure 2: BMW i3 motor map	14
Figure 3: Maximum slope and speed, speed profiles	15
Figure 4: NEDC	16
Figure 5: WLTC	17
Figure 6: Forces acting on a vehicle.	18
Figure 7: Tire deformation.	19
Figure 8: Diagram of rolling resistance.	20
Figure 9: Effective rolling radius.....	22
Figure 10: Drivetrain layout.	23
Figure 11: Power needed to motion and power available.	24
Figure 12: Inverse of acceleration	25
Figure 13: Cell types.....	26
Figure 14: Kokam pouch cell.	27
Figure 15: 2nd kinematic model structure	30
Figure 16: Backward approach model scheme.....	32
Figure 17: Backward approach model in Simulink.	33
Figure 18: Vehicle block from outside.	34
Figure 19: Vehicle block from inside	34
Figure 20: Wheel block.	35
Figure 21: Dynamic block.	36
Figure 22: Vertical force block.....	38
Figure 23: Front wheel vehicle load shift layout	38
Figure 24: WLTC actual speed vs reference speed.	40
Figure 25: WLTC speed comparison.....	41
Figure 26: Motor block.....	41
Figure 27: Motor block from inside.	42
Figure 28: Motor map.....	42
Figure 29: Motor efficiency map.....	43
Figure 30: Controller.	45
Figure 31: Battery block from outside.....	47
Figure 32: Battery block from inside.....	47
Figure 33: Vertical view of battery block.....	48
Figure 34: Thermal model.	49
Figure 35: Thermal model of 2nd order.	50
Figure 36: Transfer function.....	52
Figure 37: Temperature vs time for different values of current.	53
Figure 38: Thermal battery saturation's coefficient.....	54
Figure 39: Cell model.	54
Figure 40: Battery pack block.	56
Figure 41: OCV vs DoD.....	56
Figure 42: Electric circuit model of the cell.	57
Figure 43: Renault Zoe.	61
Figure 44: Zoe motor electric power Torque map.....	64

Figure 45: Renault Zoe evaluated performance.	66
Figure 46: CS Motor map.	69
Figure 47: CS Performance.	71
Figure 48: CS NEDC range.	72
Figure 49: CS NEDC range and SoC.	73
Figure 50: CS WLTC range.	74
Figure 51: CS WLTC range and SoC.	75
Figure 52: CS reference cycle.	76
Figure 53: CS SoC and Current for Repeated reference cycle	76
Figure 54: Simulink - Regenerative braking.	77
Figure 55: Simulink - No regenerative braking.	77
Figure 56 :CS NEDC range with and without regenerative braking.	78
Figure 57: CS WLTC range with and without regenerative braking.	79
Figure 58: CS temperature and speed.	80
Figure 59: Matlab - Run.	81
Figure 60: Matlab - Vehicle.	82
Figure 61: Matlab - Motor.	83
Figure 62: Matlab - Battery.	84
Figure 63: Matlab - Thermal model.	85
Figure 64: Simulink - Overview.	86
Figure 65: Simulink - Multiport switch.	87

1 INTRODUCTION

One of the most cause of concern about the environment, in recent years, is the global warming due to the greenhouses effect. To limit the global warming worsening, several agreements between most of the countries in the world were stipulated.

On June 4th, 1992 the United Nation signed the United Nations Framework Convention on Climate Change [1], with the objective to stabilize greenhouse gas concentrations in the atmosphere at a level that would prevent dangerous anthropogenic interference with the climate system. In 1997 was signed the Kyoto Protocol [2] that established legally binding obligations for developed countries to reduce their greenhouse gas emissions in the period 2008–2012. In 2015 the Paris Agreement [3] was adopted, governing emission reductions from 2020 on through commitments of countries in Nationally Determined Contributions, lowering the target to 1.5 °C. The Paris Agreement entered into force on 4 November 2016.

For what concerns in the specific the European Union countries, reading a communication [4] to the to the European parliament: “Climate change is a serious concern for Europeans. The current changes in our planet's climate are redrawing the world and magnifying the risks for instability in all forms. The last two decades included 18 of the warmest years on record. The trend is clear. Immediate and decisive climate action is essential”. One of the actions needed to reduce the climate exchange is an Energy Union Strategy and finalizing a modern, advanced and cost-effective regulatory framework to achieve its 2030 greenhouse gas reduction targets and its clean energy transition.

Focusing on the automotive world, the actions against the global warming are translated in a series of emission regulation that every car manufacturer must accomplish. From 2021, phased in from 2020, the EU fleet-wide average emission target for new cars will be 95 g CO₂/km. This emission level corresponds to a fuel consumption of around 4.1 l/100 km of petrol or 3.6 l/100 km of diesel. [5]

From 2019 on, the penalty will be €95 for each g/km of target exceedance. The penalties are quite high, FCA has already paid for an excess of pollutants. [6], Tesla and Fiat-Chrysler (FCA) recently reached a deal to pool their fleet together in Europe for the purpose of the latter avoiding emission requirement fines. It was first reported to be worth a few hundred million dollars, but FCA now says that it will pay Tesla up to \$2 billion for the emission credits.

The restriction in the further years will be even higher: [7], Cars: 15% reduction from 2025 on and 37.5% reduction from 2030 on. Since the Electric vehicle emission is of 0 g of CO₂, it is valid solution to the traditional, more pollutant, mobility, in order to reduce the greenhouses gasses, accomplishing therefore the increasingly stringent pollutant targets and to prevent car manufacturers to pay to high penalties.

Due to the abovementioned reasons the electric mobility is expanding at a rapid pace. In 2018, the global electric car fleet exceeded 5.1 million, up 2 million from the previous year and almost doubling the number of new electric car sales [8]. This new trend leads the mostly of the car manufacturers to address the technical research to the electric powertrain, in this new context of development is oriented the thesis work.

1.1 MOTIVATION AND OBJECTIVE OF THE THESIS

The thesis is carried out in the environment of a design of a fully electric vehicle, the purpose of the thesis is to model and simulate the longitudinal dynamic behavior of any electric vehicle, furthermore the model will be used to provide useful information for the vehicle in development as the vehicle range, in the standard driving cycles, and the performance.

However, several dynamic models are available for traditional cars, because for more than a century, cars are manufactured with an internal combustion engine, therefore plenty of research and studies about the longitudinal dynamic of the traditional vehicle are available [9], this model cannot be used for electric vehicles.

The electrical vehicles differ from the traditional cars, the main changes concern the motor and the energy storage. They have a different kind motor, no more an internal combustion engine but an electric motor, the traction torque is provided in a different manner. The energy storage is composed by a battery pack and no more by a fuel tank.

Hence, the longitudinal dynamic behavior of the electric vehicle will differ from the traditional cars, the main reasons are: a different traction delivery, the lack of need of a gearbox, due to the battery pack a different vehicle layout and weight distribution.

In recent years appeared in literature some dynamic models for electric and hybrid vehicles; about the founded researches [10], [11], [12], is possible to say that the former [10] is mostly focused on hybrid co-simulation, the research [11] is developed in specific software environment, and the last work [12] is aimed to the development of electric powertrain. My thesis work differs from the abovementioned academic works because is focused on the battery pack modelling and is developed in the Matlab-Simulink environment.

1.2 THESIS STRUCTURE

The thesis will be divided in two main chapters: the forward approach model (Chapter 2) and the backward approach model (Chapter 3), as suggest the chapter titles the main differences between them are the logic exploitation of the speed profiles, in the former, the speed profile is imposed to the vehicle, in the latter, instead, the model dynamic behavior takes into account a driver that tries to follow the selected cycle.

The following (Chapter 4) shows the results of the model with as reference the Renault Zoe, while (Chapter 5) will collect the results of the study case. A user guide with the model instructions is present in (Chapter 6), the last (Chapter 7) is devoted to the conclusion.

2 FORWARD APPROACH MODEL

2.1 INTRODUCTION

The objectives of this model are: to realize a helpful tool kit to design a battery pack of a full electric vehicle and to give a preliminary evaluation of the performance and vehicle range during the standard cycles NEDC and WLTC. Furthermore, will be exploited to pass to the backward approach model information about the energy consumption necessary to complete a standard driving cycle.

The principles of the model are based on the evaluation on the dynamic characteristics of the vehicle, that are translated in battery parameters needed for the achievement of chosen vehicle performance.

The model has a forward approach: the speed of the vehicle, read during the driving cycles, is translated into power consumption. The vehicle, in this approach, follows precisely the imposed speed cycle. The development of the model was possible thanks to the Matlab environment.

2.2 THE MODEL STRUCTURE

The model is divided in two parts: a mechanical part and an electrical one.

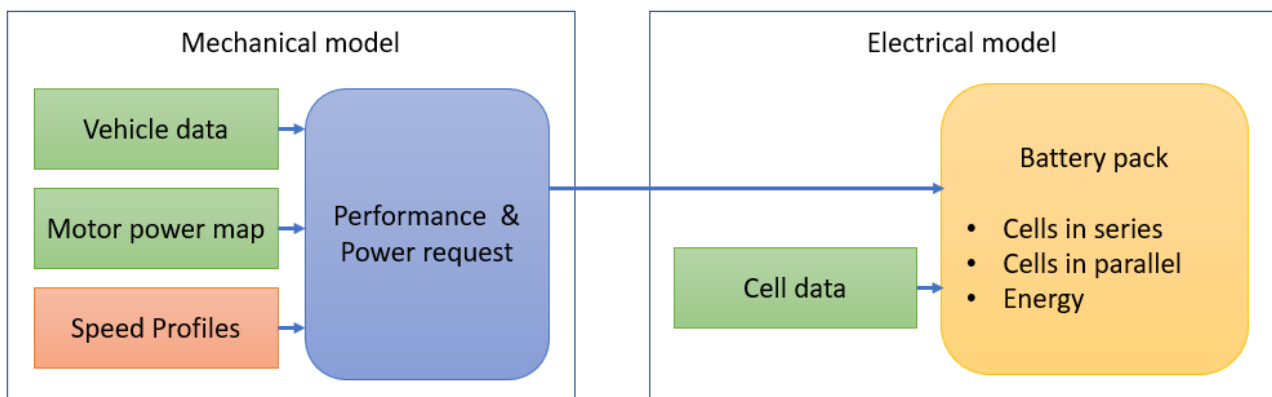


Figure 1: Forward approach model structure.

As represented in the *Figure 1* the mechanical model receives as inputs vehicle and motor characteristics, which combined with speed profiles and dynamics equations deliver as results vehicle performance and power request.

The electrical model receives as inputs cell data and the results of the previous model. The final output is the battery pack design.

In the next paragraphs will be described how each block works, every block has a correspondent .mat file of the Matlab model.

2.3 THE MECHANICAL MODEL

This model exploits the longitudinal dynamic equations in order to evaluate vehicle performance, and power consumption. Will be introduced several equations, some of them will be exploited also in the backward approach model.

2.3.1 Vehicle data

This file collects all the needed vehicle data necessary to compute the power needed to motion for each imposed speed cycle.

The main input data are below listed.

Vehicle data

- vehicle mass m
- drag coefficient c_x
- transversal surface S

Tire data

- wheel rim diameter D
- tire width W
- aspect ratio AR

Other vehicle data will be added along the thesis, every time they will be needed.

2.3.2 Motor power map

The motor map represents the power and torque values vs the engine speed, an example of electric motor map of a BMW i3 [13] is showed in Figure 2.

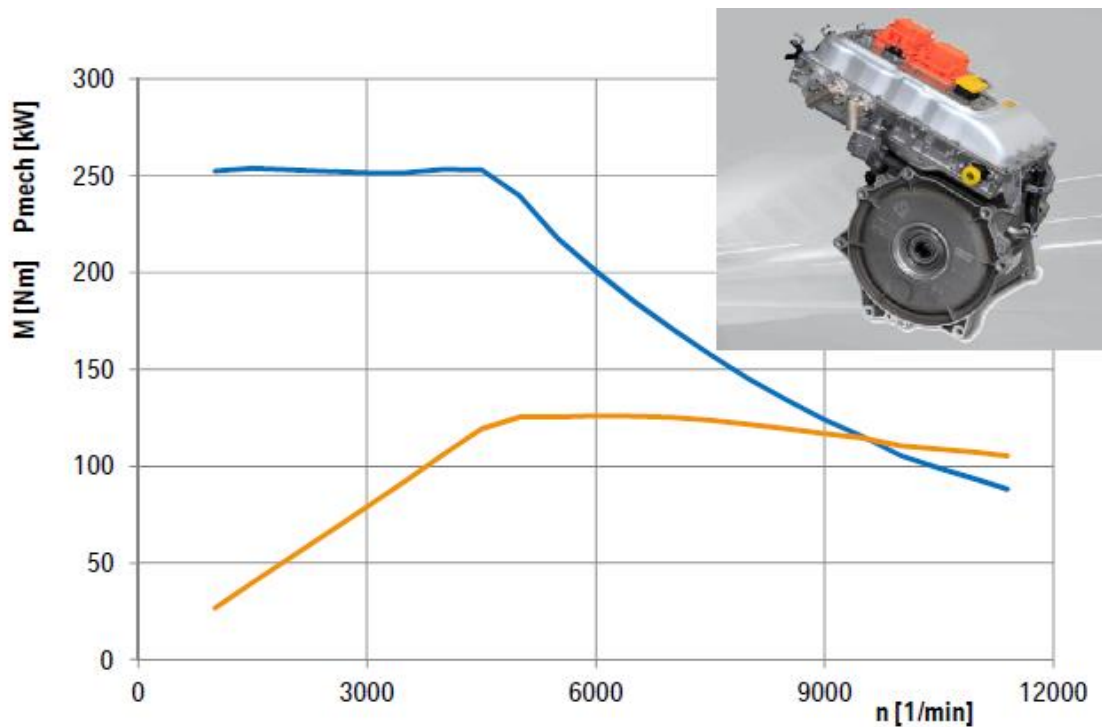


Figure 2: BMW i3 motor map

Is clear to note that electric motor has the maximum torque already available for low value of engine speed, the maximum torque is held for a certain speed range and then starts to decrease due to the induced back electromotive forces (BEMF) [14].

In the forward model the motor map is used to evaluate, at a preliminary stage, the vehicle performance.

2.3.3 Speed profiles

A series of speed profiles are used to evaluate power needed to motion for different cases.

To evaluate the most demanding power conditions the two speed cycles, showed in the below picture, are considered.

- Maximum speed cycle.
- Maximum slope cycle: 22 % $a = 1.5 \text{ m/s}^2$ [15], Data chosen from fiat standard used to design the first gear of ICE.

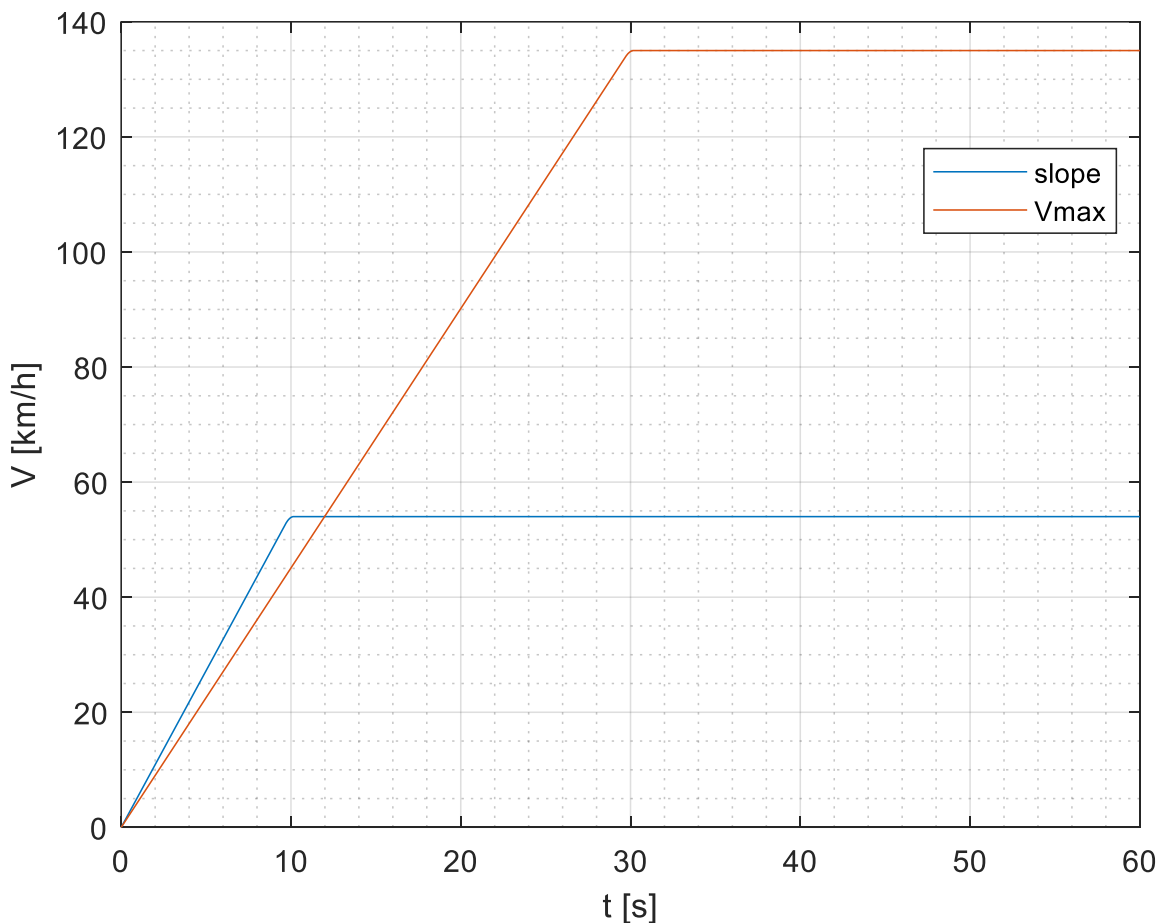


Figure 3: Maximum slope and speed, speed profiles

Furthermore, two driving cycle are evaluated:

- NEDC
- WLTC

the New European Driving Cycle (NEDC) and the Worldwide Harmonised Light Vehicle Test Cycle (WLTC), which will refer to the cycle for class 3 vehicle of the Worldwide Harmonised Light Vehicle Test Procedure (WLTP).

The former cycle is no more used, it was substituted by the WLTC starting from the 1st September of 2017 [16]. These cycles are not only used for the evaluation of power request to motion but also for the vehicle range.

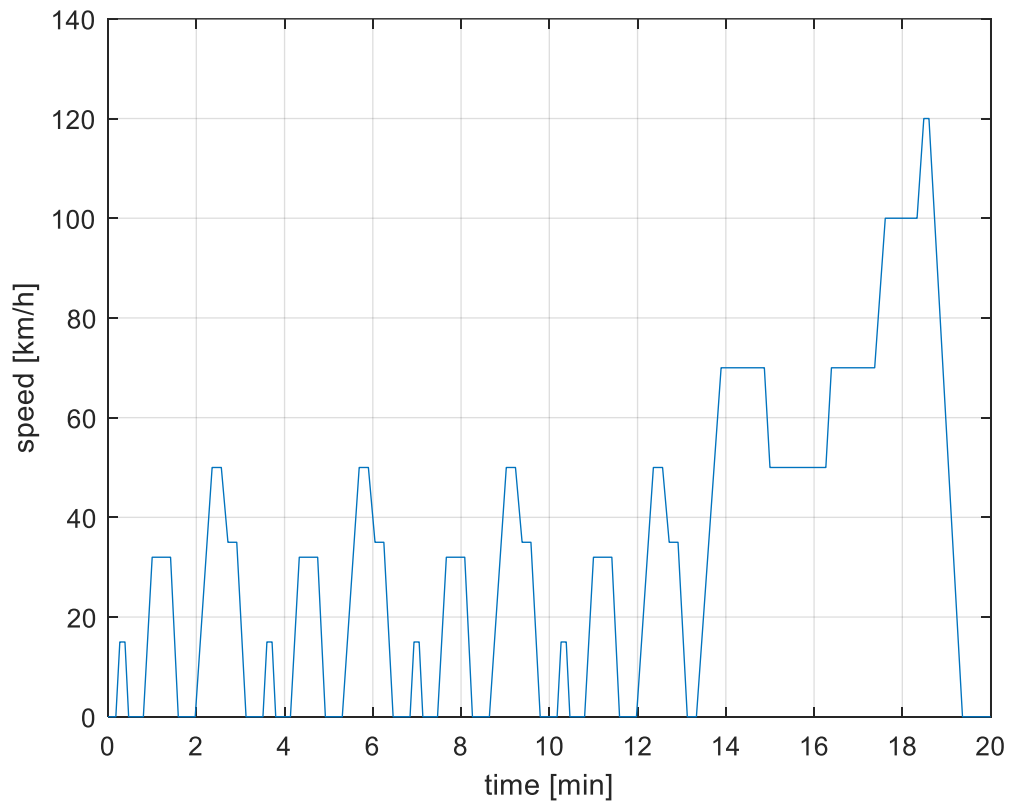


Figure 4: NEDC

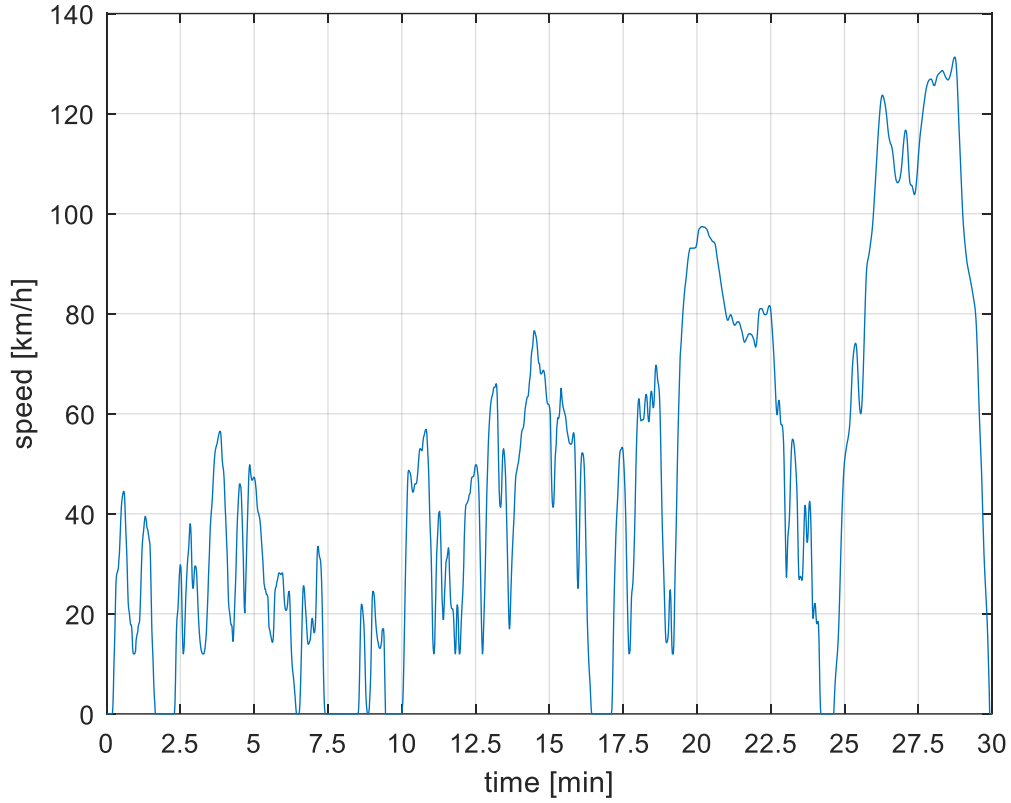


Figure 5: WLTC

These speed cycles are exploited to evaluate, as a first approximation, the vehicle range, and to compute the energy consumption needed to calibrate the proportional integrative controller of the backward approach model, that will be introduced in the next chapter.

2.3.4 Performance & Power request

This section illustrates and describes all the equations necessary to compute the power consumption and the vehicle performance.

Power needed to motion

The power needed to motion is evaluated thanks to the following formula [17], [18]:

$$P_n = F_r v + m_e \frac{dv}{dt} v \quad (1)$$

Where:

- F_r [N] is the sum of all resistance forces,
- v [m/s] is the vehicle speed,
- m_e [kg] is the equivalent mass.

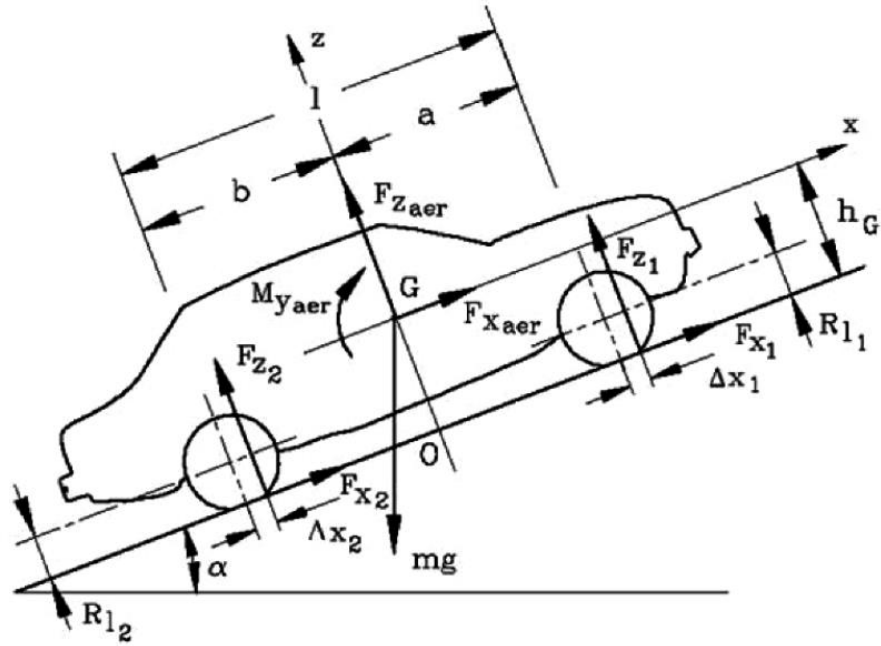


Figure 6: Forces acting on a vehicle.

F_r collects all the resistance forces, that will be described below.

Climbing force:

$$F_{climb} = mgsin(\alpha) \tag{2}$$

Where:

- m [kg] is the vehicle mass,
- g [m/s^2] is the gravity acceleration,
- α represents the slope of the road.

Aerodynamic drag resistance:

is the component of the aerodynamic force that opposes the motion of the body along the direction of the vehicle speed. The aerodynamic drag is the sum of three terms: friction drag, shape drag and induced drag.

The friction drag is the resultant of the tangential forces acting on the surface, its contribution to the total drag is on the order of 10% of the total aerodynamic drag.

The induced drag is the component of the aerodynamic drag created by the lift generation, since for the road vehicles the lift is neglectable, the induced drag has no contribution on the total drag resistance.

The shape drag is the remaining drag resistance that is not friction drag neither induced drag, it is mainly due to the wake that is created in the rear part of the vehicle.

$$F_{aero} = \frac{1}{2} \rho c_x S v^2 \quad (3)$$

Where:

- ρ is the density of the air, typically has the value of 1.3 Kg/m^3
- c_x represent the drag coefficient of the vehicle
- S is the projection of the transversal surface of the vehicle, including the wheels, respect the motion direction, typically values are around 2.5 m^2

Rolling resistance:

Is the force that is caused by the deformability of the tire and of the road. However, the road can be approximated as undeformable, it cannot be considered the same for the tire.

The energy dissipation that happen during the wheels motion can be so explained: the portion of the tire that enter in contact with the road is compressed, when that portion of tire will exit the compression zone, it will spring back to its initial shape, to produce this energy some energy will be wasted.

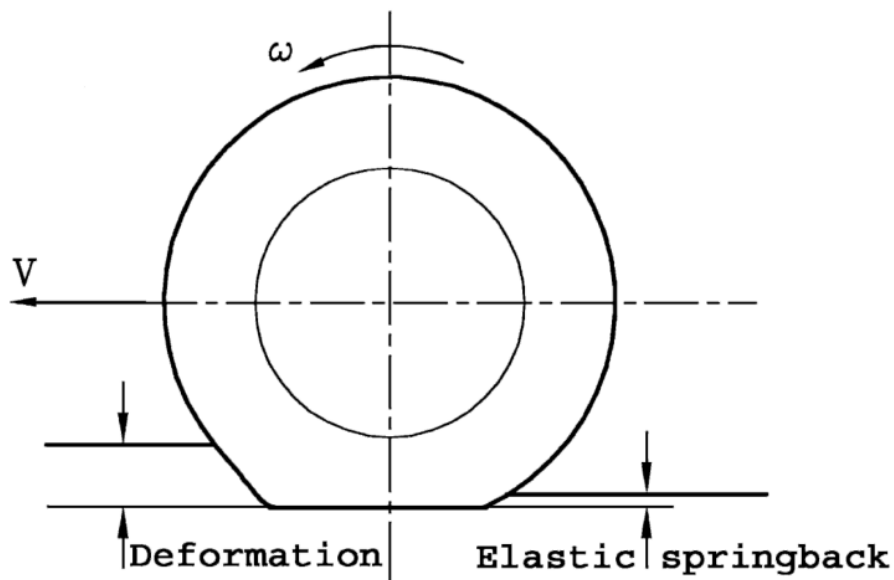


Figure 7: Tire deformation.

The rolling resistance is evaluated experimentally through laboratory testing.

$$F_{rol} = mg \cos(\alpha) [f_0 + kv^2] \quad (4)$$

It is interesting to note that the rolling resistance coefficients are two: f_0 and K . As shown in the below diagram Figure 8: Diagram of rolling resistance., the first coefficient approximates the static behavior for speed below the critical one, while the second coefficient represents the quadratic increases of the resistance.

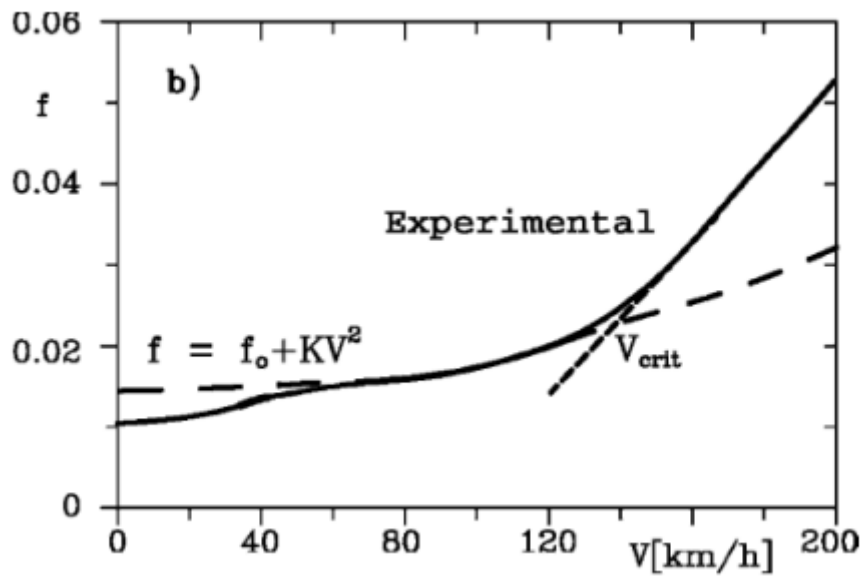


Figure 8: Diagram of rolling resistance.

To summarize: the abovementioned resistance forces can be ordered by their dependency on the speed:

$$F_r = A + BV^2 \quad (5)$$

Where:

$$A = mg[f_0 \cos(\alpha) + \sin(\alpha)] \quad (6)$$

$$B = mgk\cos(\alpha) + \frac{1}{2}\rho c_x S \quad (7)$$

The second term of the eq. (1) is represented by the inertia forces multiplied by the speed, the inertia forces is so expressed:

$$F_{in} = m_e \frac{dv}{dt} \quad (8)$$

The equivalent mass of the vehicle can be so subdivided:

$$m_e = m + \frac{4J_w}{R_e^2} + \frac{J_m i^2}{R_e^2} \quad (9)$$

where:

- m : vehicle mass
- J_w : wheel inertia
- R_e : effective wheel radius
- J_m : electric motor inertia
- i : transmission index between the angular motor speed and the wheel speed.

For a pneumatic tire an effective rolling radius R_e can be defined as the ratio the vehicle v speed and the tire angular speed Ω :

$$R_e = \frac{v}{\Omega} \quad (10)$$

As shown in the below Figure 9, the effective rolling is bigger than the loaded radius and smaller than the unloaded radius: the $R_l < R_e < R$.

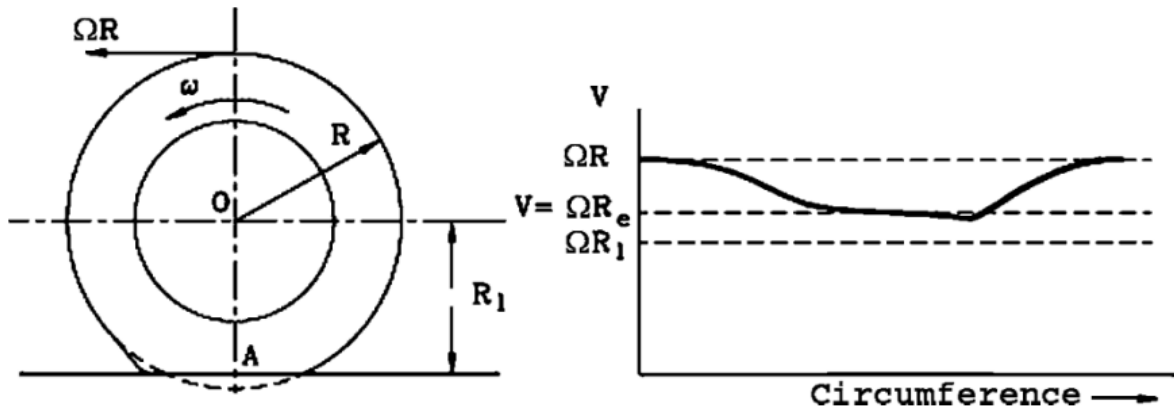


Figure 9: Effective rolling radius.

For radial tires the effective rolling radius is usually 98% of the unloaded radius R .

The unloaded radius can be found from the tire technical data, applying the following equation:

$$R = (25.4 * 0.5 * D + \frac{AR}{100} * W) \quad (11)$$

Where:

- D is the Rim diameter expressed in inches
- AR is the aspect ratio expressed in percentage
- W is the tire width in millimeters.

Coning back on the eq. (9) is not considered, on the right side of the equation is possible to notice that the inertia terms represented are the wheel inertia J_w and the motor inertia J_m , is not present the transmission inertia, for two reasons: the contribution on the overall equation is quite small, therefore negligible and also because the data is difficult to collect.

The transmission index (or ratio) is calculated as follow:

$$i = \frac{n_{max}\pi R}{30 v_{max}} \quad (12)$$

Where:

- n is the motor angular speed expressed in rpm.

2.3.4.1 Efficiencies

For sake of simplicity and for the lack of data, the efficiencies are considered constant and the values have been chosen, searching in literature [19], for their reasonability.

- Transmission η_t
- Electric motor + inverter η_m
- Battery η_b

2.3.4.2 Power at battery level (Power request)

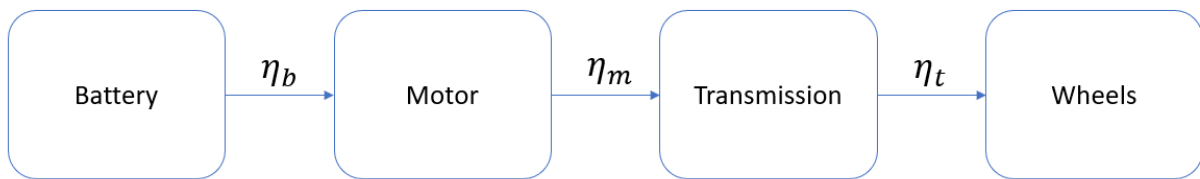


Figure 10: Drivetrain layout.

Multiplying the eq (1) for the efficiencies is possible to obtain the power at the battery level for each instant of the speed profiles [20]:

$$P_b = \eta_t \eta_m \eta_b P_n \quad (13)$$

2.3.4.3 Acceleration (Performance)

The power available to accelerate the vehicle is derived from the following equation [21] [17]:

$$P_a - P_n = \frac{dT}{dt} \quad (14)$$

- P_a is the available Power at the wheels, it is derived from the motor power map:

$$P_a(n) = \eta_m \eta_t P_m(n) \quad (15)$$

The motor power depends on the motor angular speed n , as is it possible to see in Figure 44.

- P_n is the power needed to motion, described in eq (1)
- The right term of eq. (14) represent the instantaneous variation of the kinetic energy in the time.

The kinetic energy is so expressed:

$$T = \frac{1}{2} m_e v^2 \quad (16)$$

Substituting eq. (16) in the eq. (14) is possible to extract the maximum available acceleration:

$$a_{max} = \frac{P_a - P_n}{m_e V} \quad (17)$$

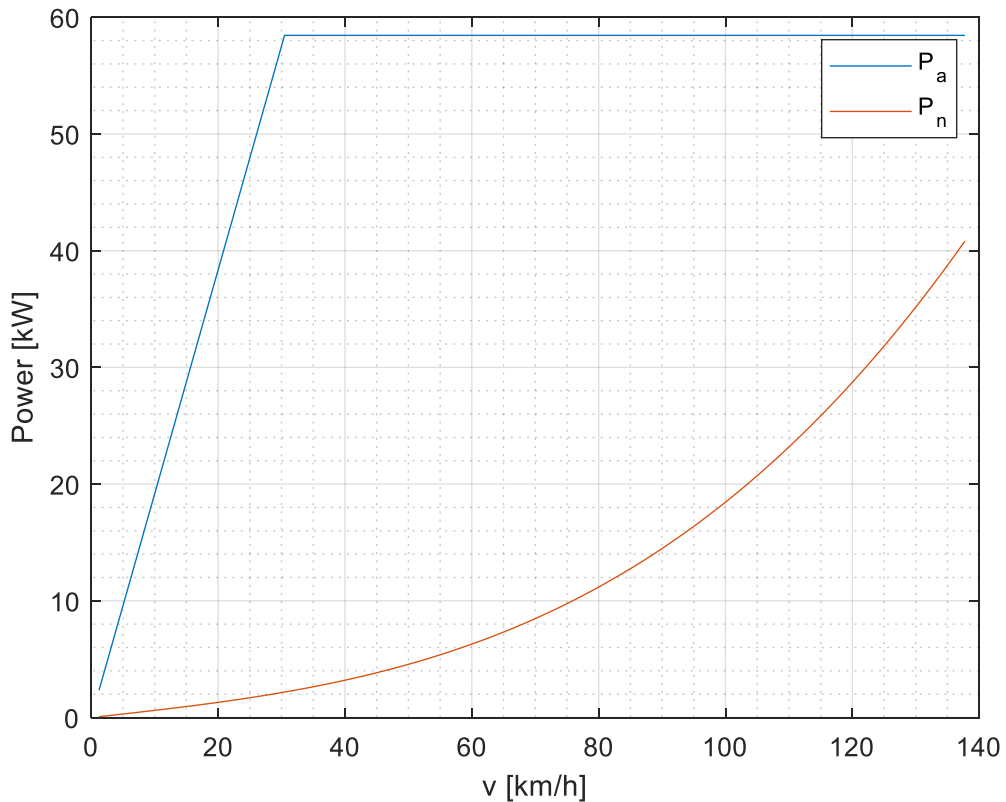


Figure 11: Power needed to motion and power available.

From the eq.(17), if the acceleration is expressed as $\frac{dv}{dt}$, is possible to derive the time needed to accelerate between to velocity:

$$t_{V_1 \rightarrow V_2} = \int_{V_1}^{V_2} \frac{meV}{Pa - Pn} dV = \int_{V_1}^{V_2} \frac{1}{a_{\max}} dV \quad (18)$$

In the below figure is plotted the inverse of acceleration against the speed, the area below the curve represent the time needed to reach the wanted speed, with the maximum acceleration available.

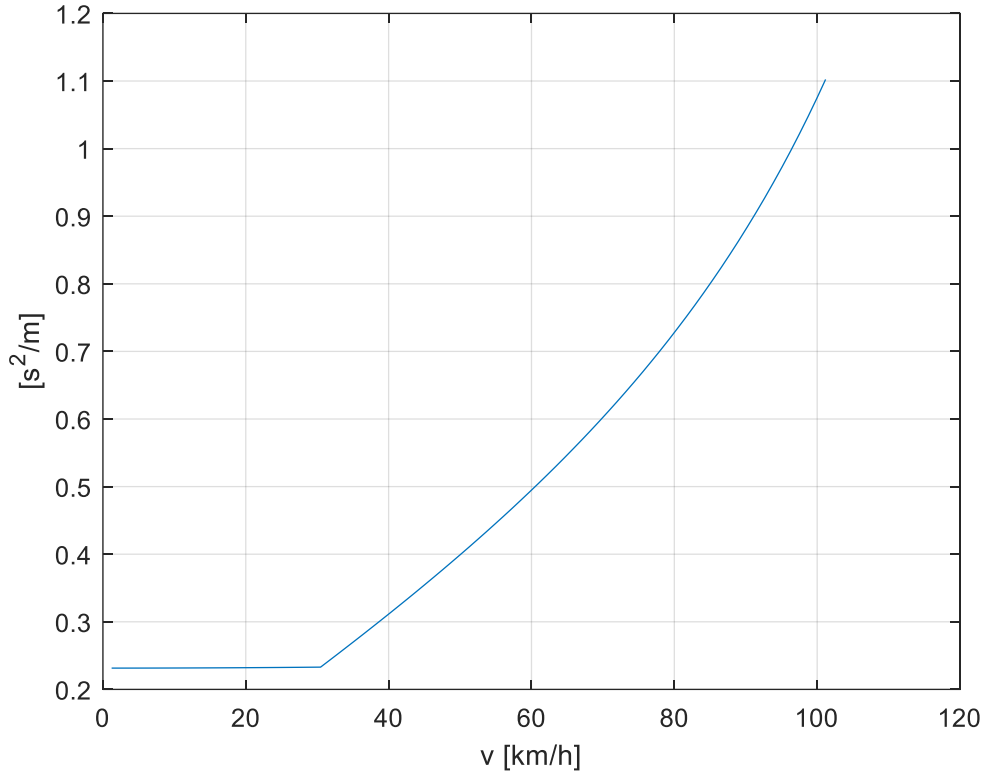


Figure 12: Inverse of acceleration

2.3.5 Energy consumption

The last output of the mechanical model in the energy consumption of the vehicle needed to complete the driving cycles, [22], the energy is calculated integrating the power needed to motion at the battery level, see the eq (13).

Hence:

$$E = \int_0^{t_f} P_b dt \quad (19)$$

2.4 THE ELECTRICAL MODEL

The aim of this model is to design a battery pack suitable for the studied electric vehicle.

The design is achieved exploiting the power and energy values that will be retrieved from the previous model, these values will be merged with the selected cell data, the final output is the battery pack design.

2.4.1 Cell

In order to design the battery pack is necessary to select the type of cell that will be used.

The cell type used for the electrical vehicle battery pack market is the lithium ion one, because guarantee the best performance in terms of power and energy density. [23]

[24] Rechargeable lithium batteries come in a variety of configurations, physical sizes, and capacity ratings. There are three basic configurations within the industry for lithium chemistry.

				
Features	Cylindrical	Prismatic	Polymer	
Energy Density	●	◐	○	● Best ◐ Better ○ Average ◑ Poor ● Worse
Standard Sizes	●	○	◑	
Cost/WH	●	○	○	
Thin Profile	◑	◐	●	
Low Weight	◑	◐	●	
Volumetric Efficiency	○	●	◐	
Low Swelling	●	◐	◑	

Figure 13: Cell types.

The Li-Poly cell called also pouch cell, has several advantages respect more traditional Li-ion cells:

- Safer.
- Light weight, great power density.
- Better low-temperature performance.
- Excellent cycle life.

Although the Li-poly cells seems to be better respect the traditional Li-ion cells, the car manufacturer's choice for electric vehicles spread among the cylindrical and pouch cells:

[25] Tesla uses cylindrical cells, Chevrolet Bolt battery pack is composed of prismatic cells, [26] the Kia Soul's is made of pouch cells.

The cell parameters used for the case studies are from the company: [27].

The input data are reported below.

Table 1: Kokam pouch cell data.

Nominal voltage	3.7	V
Capacity	53	Ah
$c - rate_{nom}$	5	
$c - rate_{peak}$	8	
Weight	1080	g
Internal resistance	0.009	Ohm



Figure 14: Kokam pouch cell.

2.4.2 Battery pack

The result of the model will be the composition of the battery pack: number of cells in series and in parallel, the energy storage and its weight.

2.4.2.1 Cells in series

The computation of the number of cells in series is dependent on the voltage of the electrical motor, for what regards the Renault Zoe the maximum voltage is of 400 V, see Table 2, therefore the nominal one is estimated of about 355 V. The formula to compute the total number of cells in series is:

$$n^{\circ} \text{ series} = \frac{V_{bat}}{V_{cell}} \quad (20)$$

2.4.2.2 Cells in parallel

To find the number of cells in parallel are used two different criteria:

- Current criterion
- Energy criterion

The total number of cells in parallel will be the maximum value between these criteria

Current Criterion

This approach is aimed to guarantee that the discharge current of the battery guarantees the desired power.

Knowing that the electric power can be written as $P = VI$, is possible to rewrite the equation in order to find the current, necessary to maintain that level of power necessary to accomplish the studied driving cycle:

$$I = \frac{P_b}{V_{bat}} \quad (21)$$

Since a cell cannot discharge instantaneously an unlimited amount of current, there is a cell parameter that specifies how much amount of current can be discharged, this parameter is called c-rate [28].

The c-rate is a measure of the rate at which a battery is discharged relative to its maximum capacity. A 1C rate means that the discharge current will discharge the entire battery in 1 hour.

To increase the rate of discharge of a battery is possible to dispose cells in parallel, in such a way the current is distributed among the cell in parallel.

The number of cells in parallel, thanks to this criterion, will be:

$$n_c = \frac{I}{c - rate C_{cell}} \quad (22)$$

Where:

- C_{cell} [Ah] is the cell capacity

From the Table 1 is possible to see that there are two different type of c-rates, one is the peak c-rate and the other one is the nominal c-rate. The former value is used when the power delivered by the vehicle is under the highest transient condition: the maximum acceleration, while the latter value of c-rate is expressed by nominal condition such as a vehicle with a constant speed.

Therefore, for the peak c-rate value is used in the eq. (21), the maximum power achieved during the maximum acceleration. While for the c-rate nom is used the power measured during the cycle with the maximum speed.

The current values derived from the eq. (21), will be inserted in the eq. (22) allowing so to find the minimum number of cells in parallel necessary to guarantee the power delivered by the battery to the vehicle.

The energy criterion

This criterion differs from the previous ones, here the parameter to calculate the number of cells in parallel is the energy necessary to accomplish a driving cycle.

$$n_E = \frac{E_{cycle}}{V_{cell} C_{cell}} \quad (23)$$

The objective is to guarantee that the cell capacity is enough to allows the completion of a determined number of driving cycle i.e. a certain vehicle range.

To conclude, the maximum number of cells in parallel will be the highest value that comes from the current and energy criteria:

$$n^{\circ} \text{ parallel} = \max(n_C, n_E) \quad (24)$$

2.4.2.3 Battery pack weight

The net weight is computed multiplying the cell weight for the total amount of cells.

The total gross weight considers the complete module with the coolant plates. The evaluation was estimated thanks to internal data of the company FLAG and data found on the website: [29]:

- Flag prismatic cell battery pack (30 kWh per 326 kg)
- Flag pouch battery pack (40 kWh per 380 kg)
- Tesla model S battery pack (85 kWh per 540 kg)

A weighted average of the above data leads to the following experimental formula:

$$W_{tot} = W_{cell} + 35\% W_{cell} \quad (25)$$

2.5 FURTHER CONSIDERATIONS

2.5.1 Vehicle range

Knowing the battery energy and the energy needed to finish the driving cycles is possible to evaluate the vehicle range [22] :

$$Range[km] = \frac{E_{battery}}{E_{cycle}} length_{cycle} \quad (26)$$

Where the cycle length is of:

- 11 km for NEDC
- 23.25 km for WLTC

2.5.2 Motor design

In this model the power map of the motor was assumed as an input parameter. If the motor will be managed as an output of the system is possible to change the model layout as showed below:

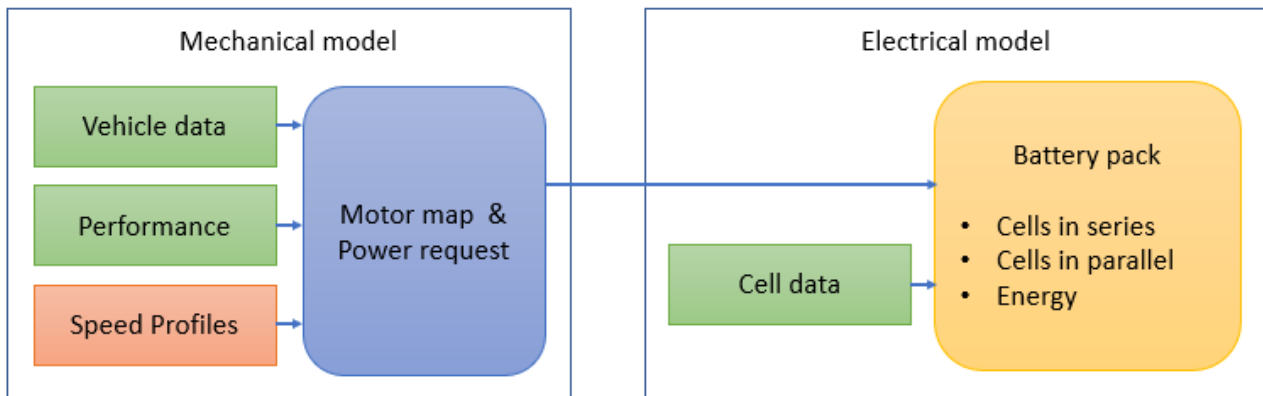


Figure 15: 2nd kinematic model structure

From the comparison between *figure 1* and *figure 11*, is clear to note that the motor map is no more an input of the system but is now an output, while the performance became an input.

The logic behind the motor map design is to increase the peak power in order to achieve fixed acceleration performance.

3 BACKWARD APPROACH MODEL

3.1 INTRODUCTION

In this chapter will be described the longitudinal dynamic model that has been realized, differently from the previous chapter, the dynamic approach to the speed cycle is of backward type, this means that the vehicle does not follow strictly the cycle speed profile, instead, through a proportional integrative controller, the vehicle tries to fill the gap between the reference speed and the actual one.

Since with the backward approach is simulated the driver, thanks to the proportional integrative controller, it describes more accurately the dynamic behavior of the vehicle.

Moreover, this backward approach is equipped with a thermal model which enables to read the battery pack temperature and eventually to cut off the current supply.

The results of the model are of dynamic type: vehicle performance and the vehicle range with two different driving cycles, and of battery control type: current amplitude, state of charge and battery pack temperature.

3.2 THE MODEL OVERVIEW

The model is implemented in the Simulink-Matlab environment. While the Matlab software collects the input data as vehicle mass, drag coefficient, motor map, and others, the Simulink extension is exploited to subdivide the vehicle in functional blocks: a vehicle block, a motor block and a battery block, furthermore, as shown in the next Figure 16, a controller simulates a driver that tries to follow the chosen speed cycle, that is illustrated on the right side of the scheme.

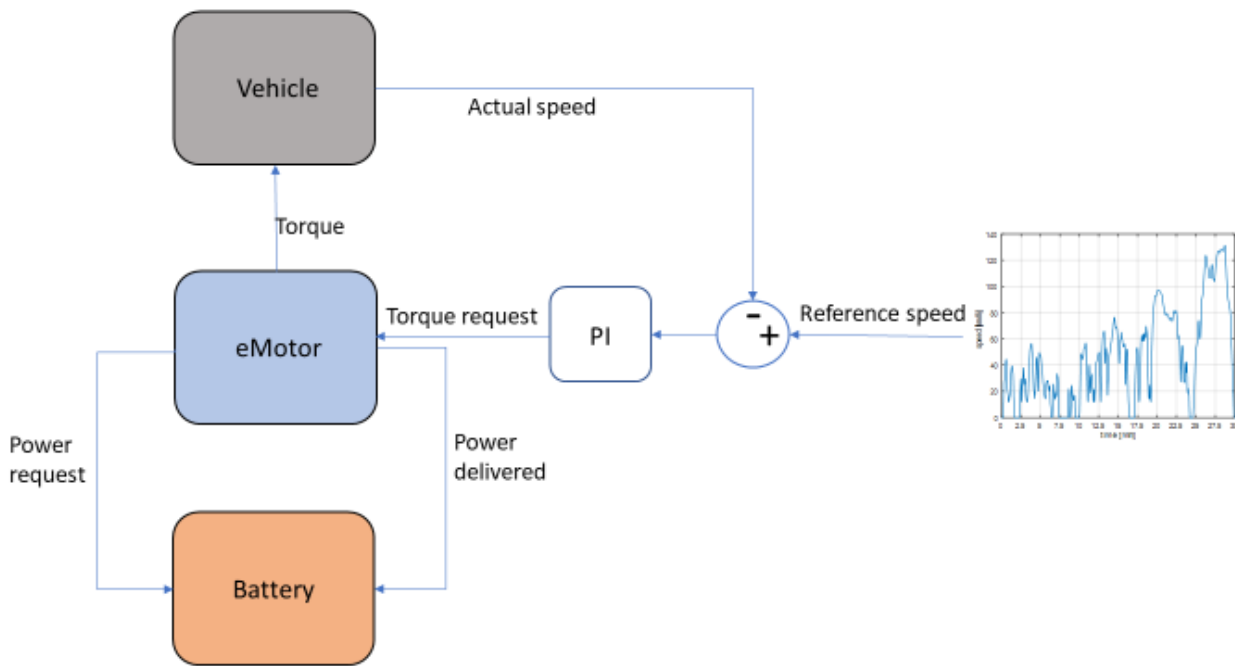


Figure 16: Backward approach model scheme.

Deepening the interactions between blocks follows that the first input of the system is the reference cycle that is compared with the vehicle actual cycle, after the proportional controller block, the speed comparison is translated into a torque request. The battery and the motor blocks interact each other through a power request from motor to battery and a power delivered vice versa. The motor and the vehicle block are linked by the torque delivered by the motor. To conclude the torque is converted into vehicle speed in the vehicle block.

The complete Simulink scheme of the model is visible in the next Figure 17, in the scheme is represented an example with a WLTC cycle engaged as reference speed cycle. Is possible to notice the range output of 23,25 km and the SoC level that is lowered, after one cycle, with a value of 91,55 %.

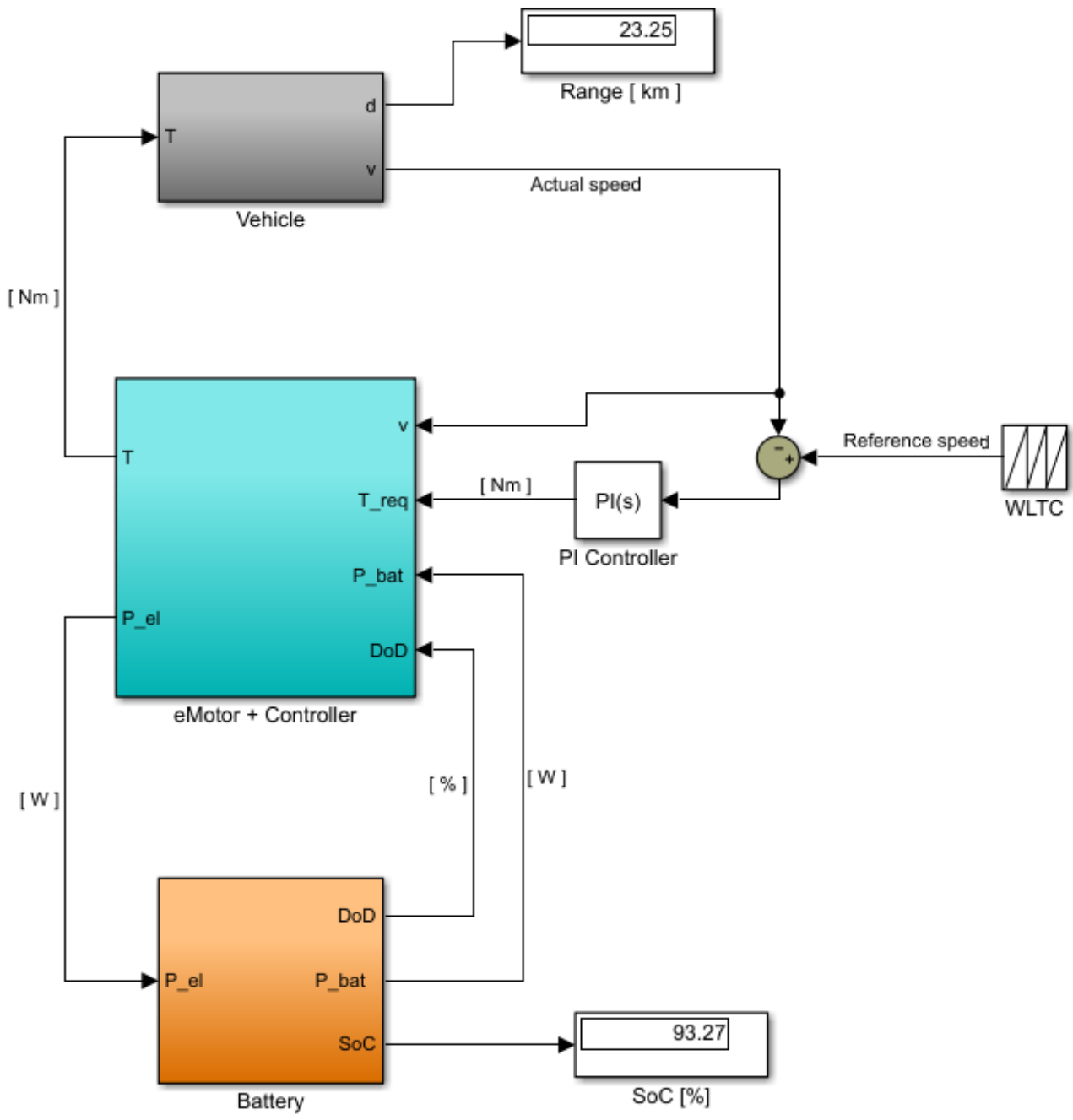


Figure 17: Backward approach model in Simulink.

3.3 VEHICLE BLOCK

The vehicle block input is the torque value coming from the motor block, the outputs are the actual vehicle speed and the distance travelled.

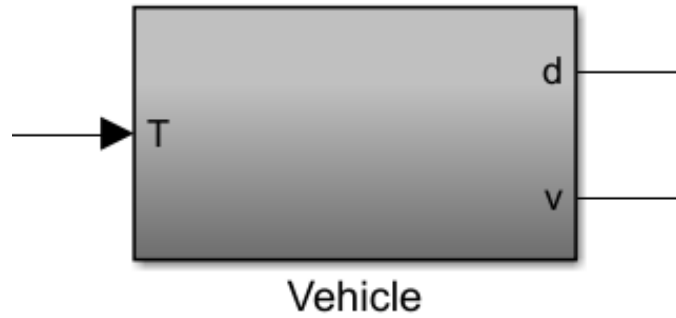


Figure 18: Vehicle block from outside.

The inside structure is showed in the below picture, the first section is dedicated to the wheel representation, the second one collects the dynamic equations that rules the motion, a third block is employed to evaluate the travelled distance.

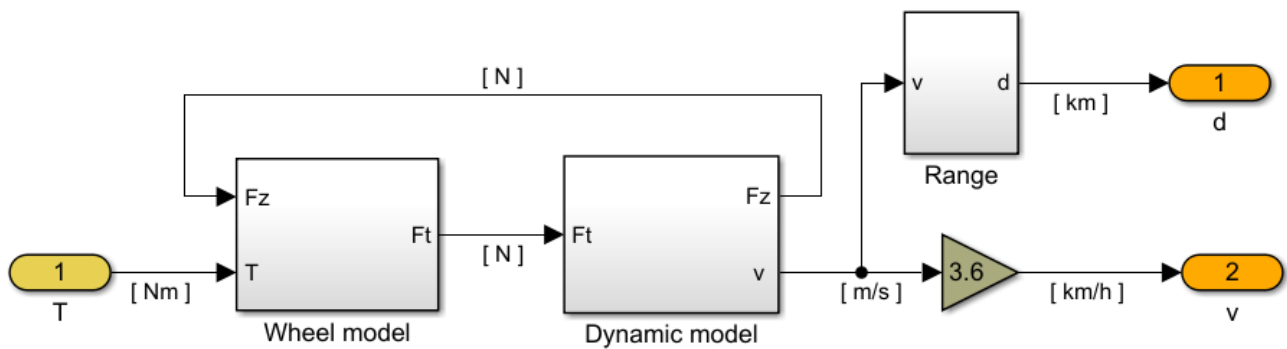


Figure 19: Vehicle block from inside

3.3.1 Wheel model

This block converts the torque into a traction force needed to move the vehicle, the wheel model is composed of a traction part that can be limited, if the torque input is too high, by the tire slip coefficient.

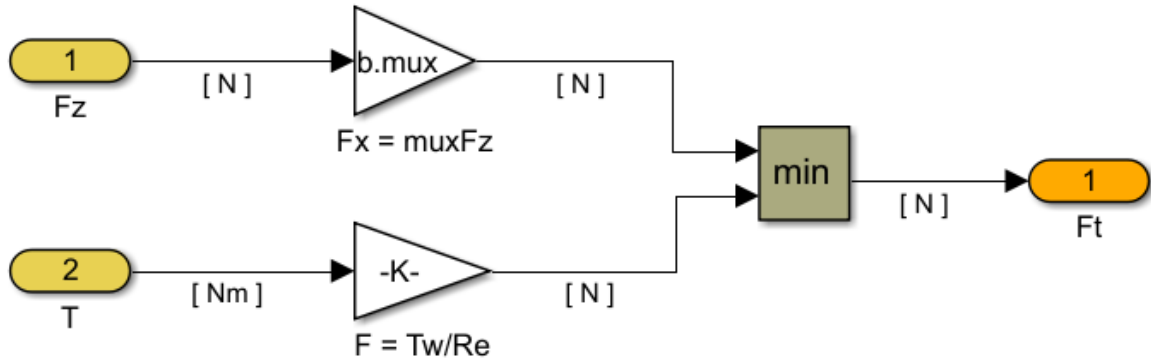


Figure 20: Wheel block.

The equation used are the following [17]:

$$F_{t_1} = \frac{T_w}{R_e} \quad (27)$$

The numerator represents the torque at the wheel, that is so evaluated:

$$T_w = \eta_t i T \quad (28)$$

Where:

- η_t is the transmission efficiency
- i is the transmission ratio
- T is the motor torque

The traction force, transmitted on the ground by the traction wheels, is limited by the weight on the traction axis times the slip coefficient of the tire, the equation that define this traction limitation is:

$$F_{t_2} = \mu_x F_z \quad (29)$$

Where:

- μ_x is the tire slip coefficient, its value is chosen as constant and is about: 0,80-1,00.
- F_z is the vertical force on the driving axis, it depends on the car weight distribution on the traction wheels and on the load shift due to the inertia force. In this model are not considered the contributions of the drag and rolling resistance forces because are not relevant for the accuracy of the model.

$$F_t = \min(F_{t_1}, F_{t_2}) \quad (30)$$

3.3.2 Dynamic model

This section describes the dynamic equation that rules the vehicle motion and weight distribution on the traction wheels. It receives as input the traction force that will subtract for the resistant forces that are computed in the dedicated block. While the vehicle speed is the output of the whole vehicle block, the vertical force will be exploited to the traction force evaluation of the previous wheel model block.

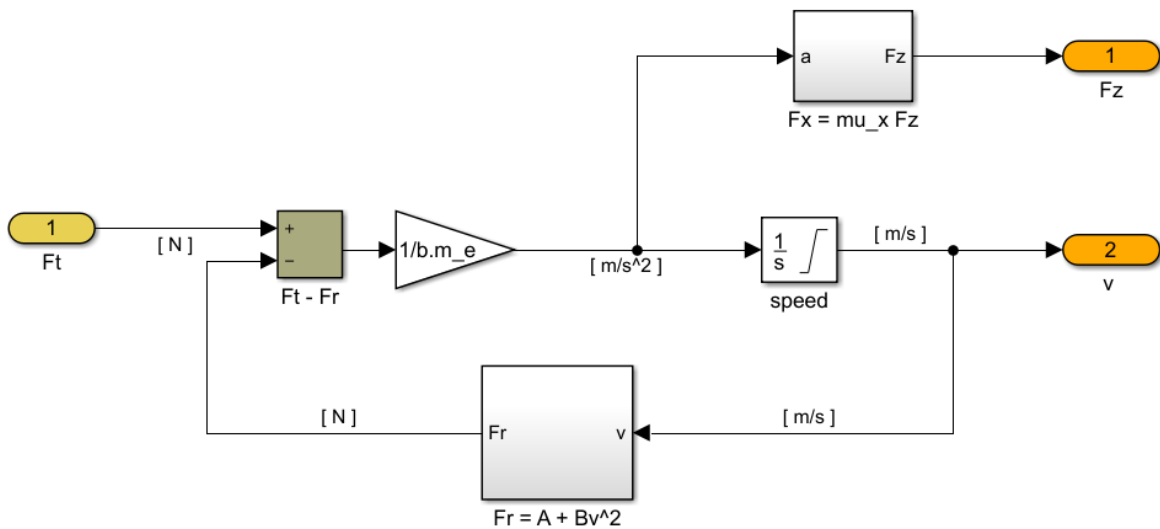


Figure 21: Dynamic block.

The acceleration of the vehicle is evaluated thanks to the 2nd Newton' Law, indeed, is possible to write:

$$F_t - F_r = m_e a \quad (31)$$

Where:

- F_t is the traction force and comes from eq (30),
- F_r is the resistant force and is calculated in eq. (5),
- m_e is the equivalent mass and is expressed in eq. (9).

Rewriting the abovementioned equation, is possible to obtain the vehicle acceleration:

$$a = \frac{F_t - F_r}{m_e} \quad (32)$$

The vehicle speed, expressed in [m/s], is obtained integrating the acceleration r:

$$v = \int_{t_0}^{t_f} a dt + v_0 \quad (33)$$

The last output of the dynamic model is the vertical forces acting on the traction wheels. This output will be employed in the previous block, see eq. (29).

There are three different vehicle configurations:

- front traction drive (FWD)
- rear traction drive (FWD)
- all wheel drive (AWD)

The model allows to choose among these three different drive layouts.

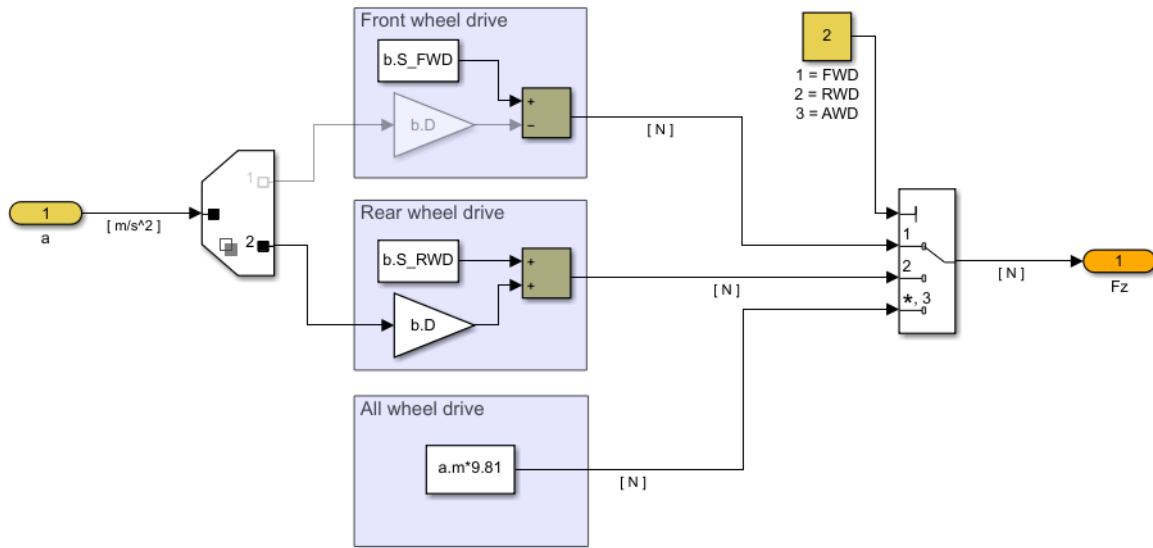


Figure 22: Vertical force block.

If the vehicle has a rear traction configuration, the load shift will be added to the vertical forces, if the configuration is of front traction type, will be instead subtracted, if the vehicle has all-wheel drive the maximum amount of traction is a function of just the slip coefficient and the vehicle mass.

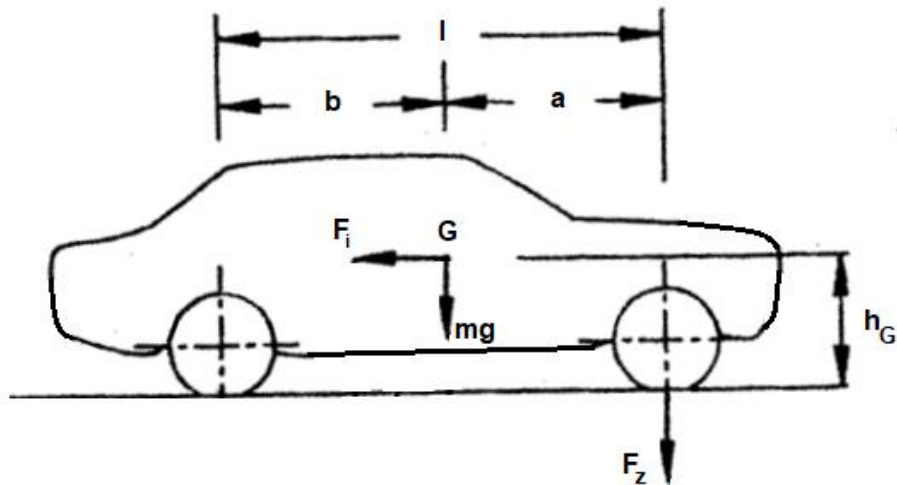


Figure 23: Front wheel vehicle load shift layout

From the Figure 23, is possible to derive the load shift on the traction axis:

Front wheel drive (FWD):

$$F_z = m \left(g \frac{b}{l} - \frac{dv}{dt} \frac{h_g}{l} \right) \quad (34)$$

Rear wheel drive (RWD):

$$F_z = m \left(g \frac{a}{l} + \frac{dv}{dt} \frac{h_g}{l} \right) \quad (35)$$

All wheel drive (AWD):

$$F_z = mg \quad (36)$$

3.3.3 Range

This block is aimed to compute the vehicle range, the distance is computed integrating the speed over the time, the result is converted from meter to kilometers dividing it by 1000.

$$d = \frac{1}{1000} \int_{t_0}^{t_f} v dt \quad (37)$$

The range block will be exploited for the evaluation of the vehicle range for the driving cycles: WLTC and NEDC.

3.4 SPEED COMPARISON

In the previous chapter were described how the torque coming from the electric motor was converted in vehicle speed, thanks to the driveline block.

The actual vehicle speed will be compared with the reference vehicle speed instant per instant, in the below Figure 24, is showed the actual speed and the reference one of a WLTP cycle.

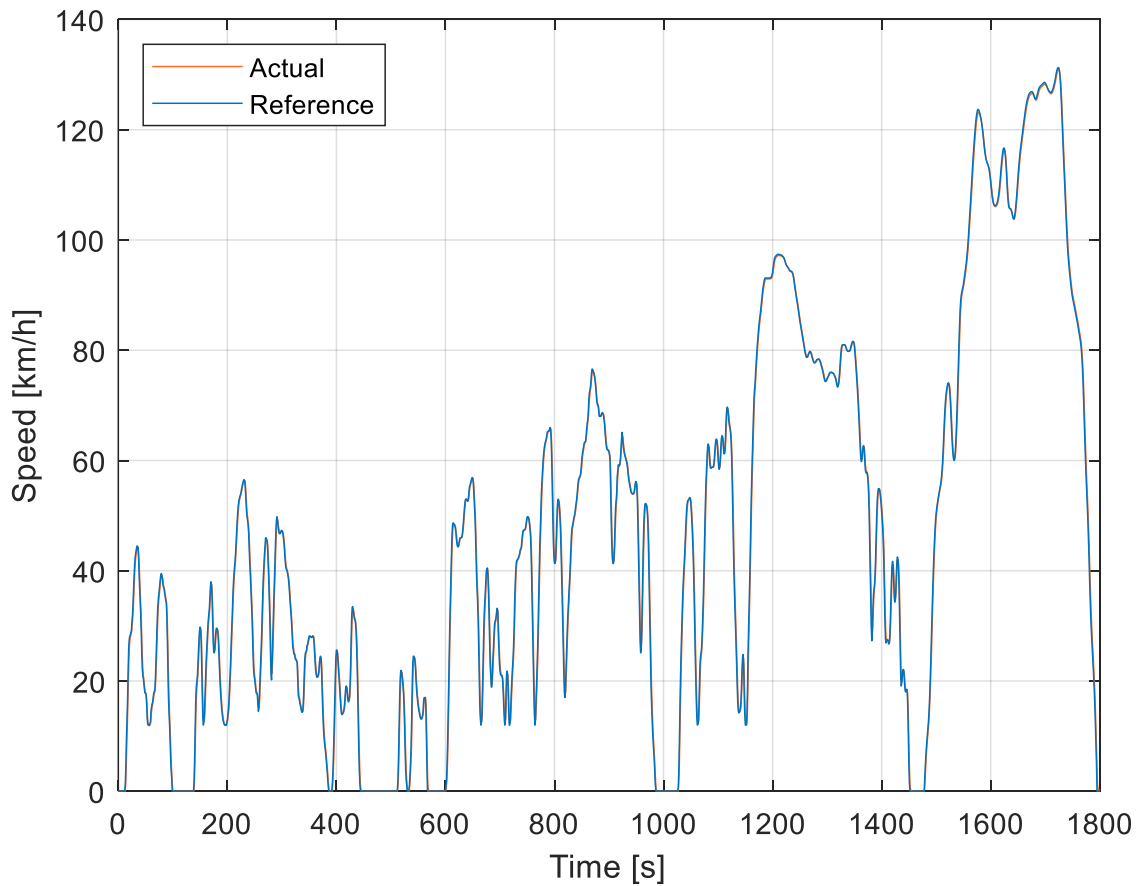


Figure 24: WLTC actual speed vs reference speed.

The differences between the two speed profiles, highlighted in the next Figure 25, will be analyzed by a proportional integrative controller that will produce as gain torque value.

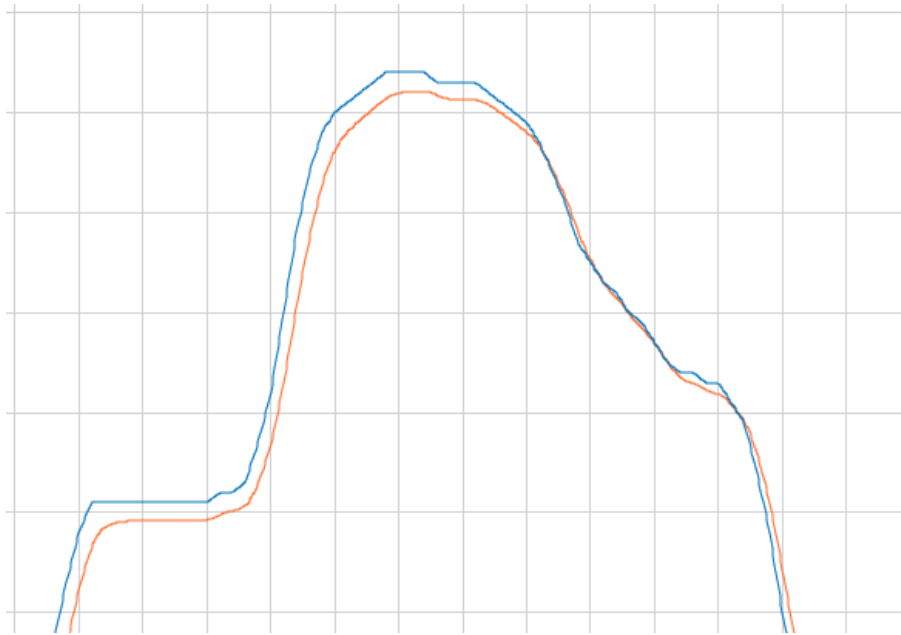


Figure 25: WLTC speed comparison.

The proportional integrative controller simulates a driver behavior and has the objective to follow the reference speed profile.

The Proportional and Integrative values have been chosen experimentally, paying attention that the torque and engine speed values of the motor map will be in acceptable range, and that energy consumption is compatible with the energy evaluated during the forward model.

3.5 MOTOR BLOCK

This block represents the electric motor and the controller that manages the battery saturations.

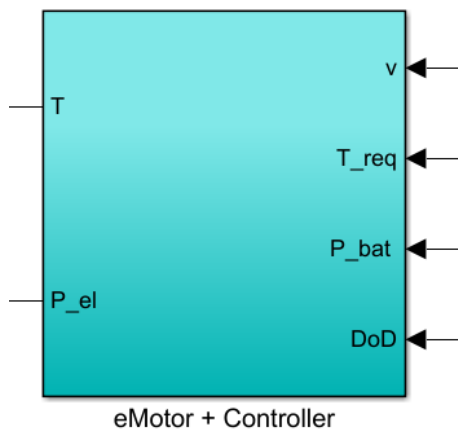


Figure 26: Motor block.

It receives as inputs from the vehicle block the actual speed, from the PI controller the torque request, from the battery the battery power and the depth of discharge, it returns to battery the electric power and sends to the vehicle block the torque.

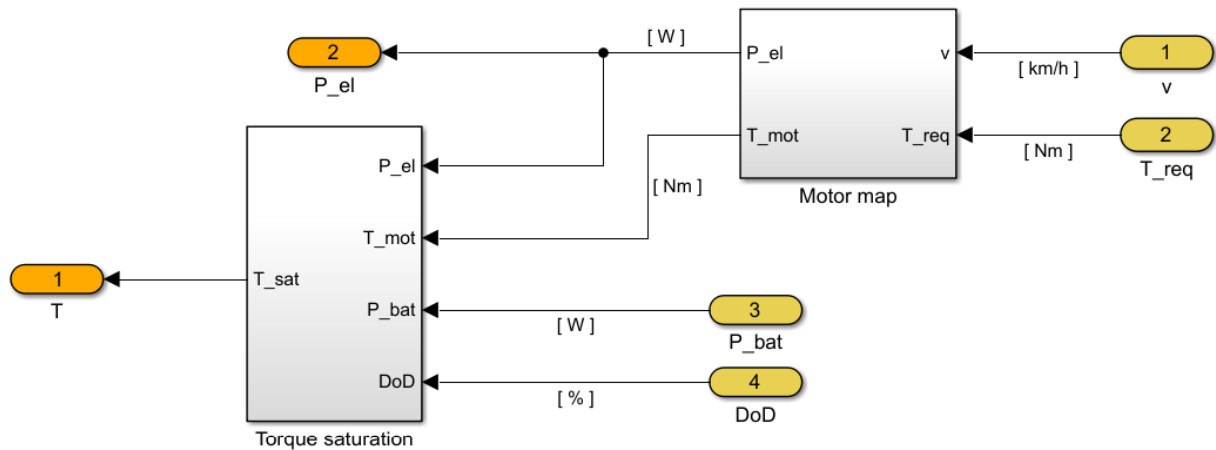


Figure 27: Motor block from inside.

3.5.1 Motor Map

The block includes two look-up tables, one table represents the torque curve of the motor, while the second one constitutes the efficiency map of the motor and the inverter, coupled together.

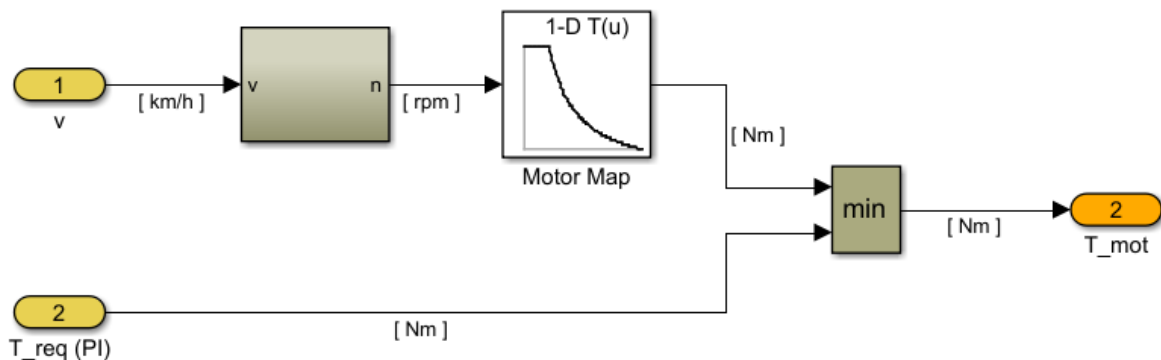


Figure 28: Motor map.

The first input of the system is the actual vehicle speed that will be converted in engine speed, through:

$$n [rpm] = \frac{30 i}{3.6 \pi R_e} v [km/h] \quad (38)$$

For each engine speed the correspondent maximum torque value will be gather from the motor map, already introduced in the Figure 44.

This torque value is compared with the gain value retrieved from the PI controller. The minimum value among them will be the Torque output value.

This torque value with the engine speed will be needed for the efficiency motor+inverter map.

The efficiency maps of the motor and inverter are joined together for sake of simplicity, the values were gathered from internal sources and were changed in order to fit the torque and engine speed range of the considered motor.

An example of motor efficiency map is showed below.

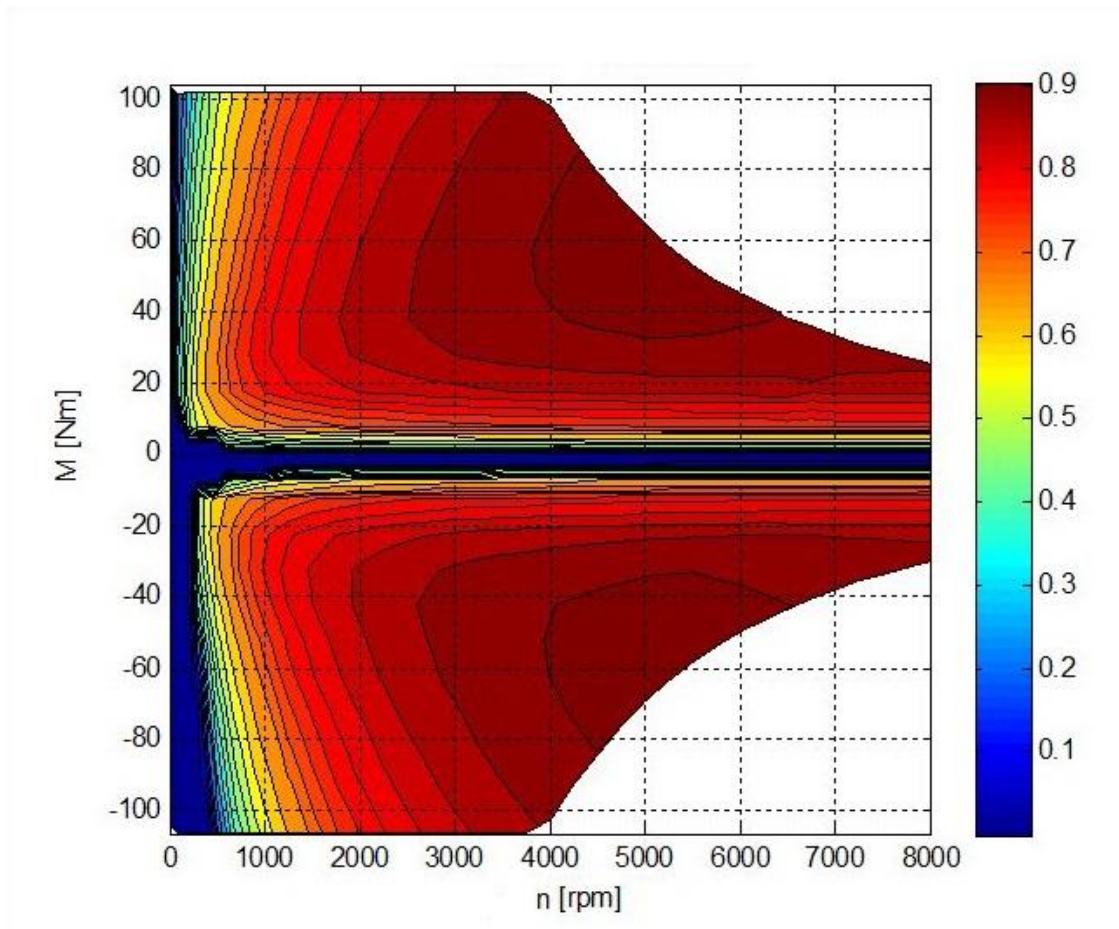


Figure 29: Motor efficiency map.

Is it clear to note that, contrary to an internal combustion engine, the efficiency range is extended also for negative values of the torque.

The negative values are due to the regenerative braking system of electric vehicles, the regenerative braking exploit the double function of the electric motor: deliver the traction acting as motor, absorbing the shaft rotation, acting as generator. During braking will be therefore possible to convert part of the braking energy and stock it in the battery pack.

Differently from the internal combustion engines, the efficiencies values of the motor are quite higher, with an average value of 90 % for a wide range for rpm and torque.

The efficiency map is represented in the model as a look up table, that for input values of torque and engine speed return an efficiency value.

In parallel with this operation, the torque is multiplied by the engine speed, obtaining so the mechanical power:

$$P = T\omega \quad (39)$$

Where ω is the engine speed expressed in [rad/s].

At this stage the objective is to derive the electrical power needed by the motor to compensate the efficiency loss of the motor.

The electric power calculation is so realized:

$$P_{el} = \begin{cases} \eta P_m, & P_m < 0 \\ \frac{P_m}{\eta}, & P_m \geq 0 \end{cases} \quad (40)$$

From the above system is possible to see that the electric power will increase respect the mechanical one when the vehicle is in traction condition, indeed is request more power to the battery respect the mechanical one. On the other hand, the electrical power will, instead, decrease during regenerative condition, limiting so the amount of energy that will recharge the battery.

In summary, in this block the inputs are the actual vehicle speed and the torque request, the output of the system will be the torque values, chosen as minimum between the torque request and the motor map value, and the electric power, that will be the input of the battery block.

3.5.2 Controller

In this block is conducted a control to limit the torque output if two condition are reached, one coming from the thermal model and one depending on the battery charge.

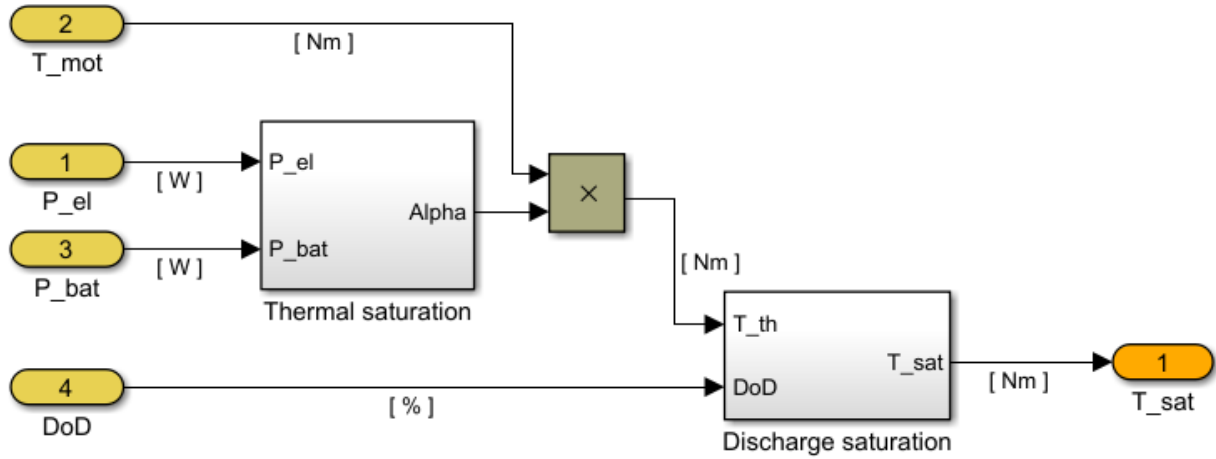


Figure 30: Controller.

Thermal saturation:

If in the battery block there is a current saturation due to an overheating of the cells, the battery power, as consequence, will be saturated and so its value will be lower respect the electric power.

A lower power coming from the battery, respect the expected one, leads to a reduction of torque output to the wheels.

The algorithm which consider the power reduction is the following:

$$\alpha = \begin{cases} 1, & P_{el} - P_{bat} = 0 \\ \frac{P_{bat}}{P_{el}}, & P_{el} - P_{bat} > 0 \end{cases} \quad (41)$$

Where, the coefficient α , which is limited for value $0 < \alpha < 1$, is exploited to calculate the saturated value of torque:

$$T_{bat} = \alpha T \quad (42)$$

The previous passage is consistence, since:

$$\frac{P_{bat}}{P_{el}} = \alpha = \frac{\omega T_{bat}}{\omega T} = \frac{T_{bat}}{T} \quad (43)$$

Where the engine speed ω have the same value, so can be cancelled out

Discharge saturation:

This section takes in analysis the current saturation due the current discharge of the battery pack. The parameter that represent the cell state of charge is called Depth of Discharge (DoD), and is expressed in percentage points, 0% means that the cell is fully charged, while 100% means that the cell is completely discharged.

When the battery Depth of Discharge reach the value of 100% the current saturation is reached, and therefore no more batter power is available. The result is that the motor will stop to provide torque to the wheels and the vehicle. Hence, the vehicle will quickly stop.

To conclude, the torque value available to the vehicle block will be the one coming from the motor map, unless there is a saturation coming from the controller.

3.6 BATTERY BLOCK

The aim of this model block is to represent the electric vehicle's battery pack.

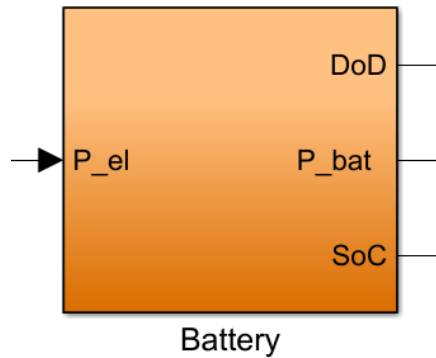


Figure 31: Battery block from outside.

The only input of the system is the electric power computed in the motor block, see eq. (40), which represents the power absorbed by the motor to guarantee the mechanical power request to motion.

The outputs of the model are the battery power, which differs from the electric power in the cases of current or thermal saturation, the depth of discharge (DoD) and the state of charge (SoC), while the former shows the amount of discharge of the battery, the latter indicates the level of charge.

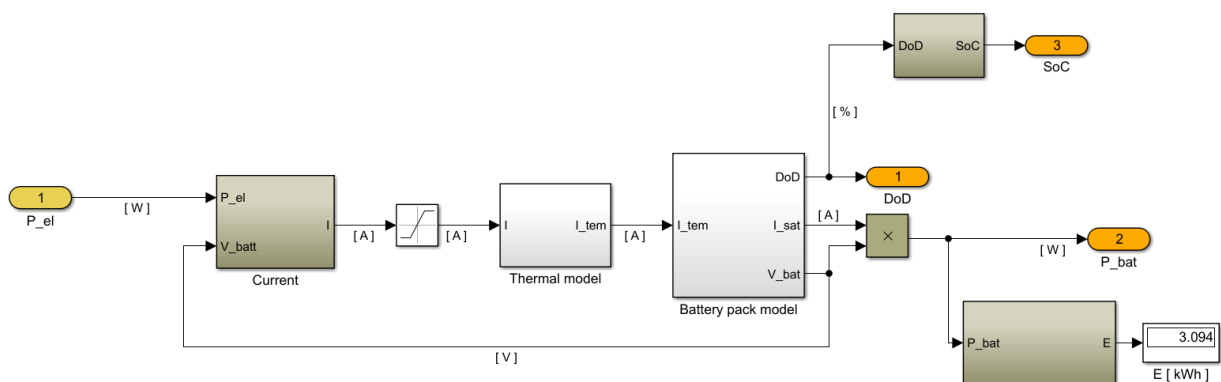


Figure 32: Battery block from inside.

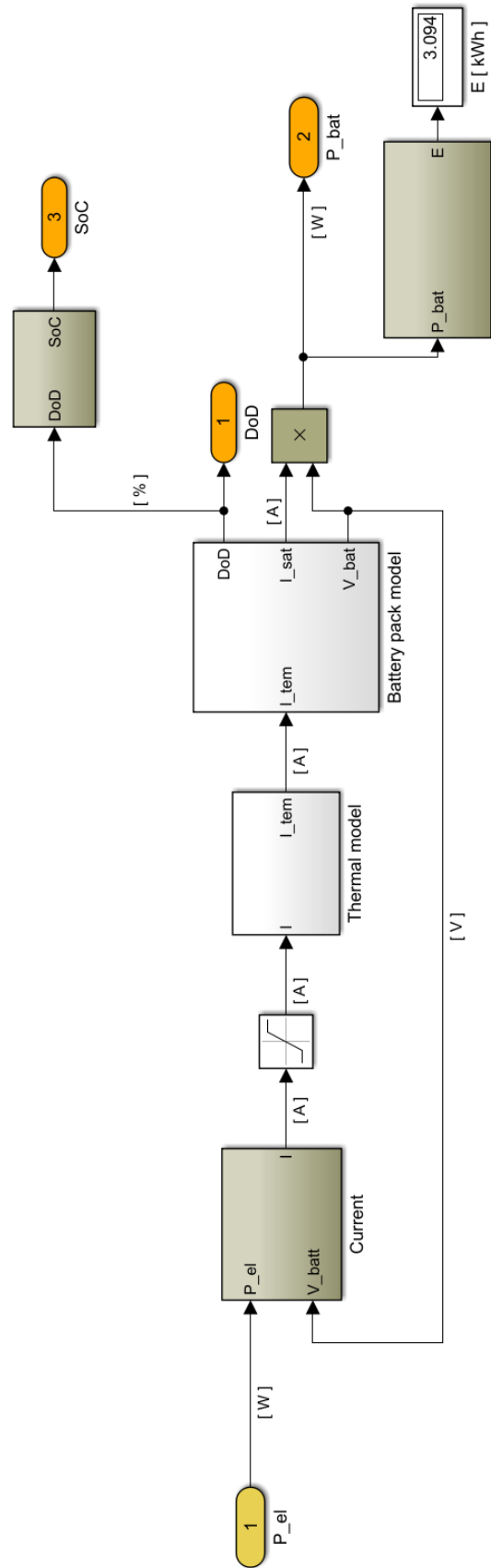


Figure 33: Vertical view of battery block.

As shown in the Figure 32 and Figure 33, is clear to note that the battery model is composed of several blocks, the first one derives the current from the electrical power input, then a saturation block allows to set limits on the positive current and the negative one (regenerative current), afterwards a thermal model evaluates the battery block temperature and eventually saturates the current, to conclude a cell model schematizes the battery cells configuration and evaluates its charge level.

Further blocks are needed to evaluate the energy consumption of the battery and to convert the depth of discharge in the state of charge.

3.6.1 Current

The first block that appear is the current one, here the electric power will be divided for the current battery voltage, coming from the Cell model, obtaining so the actual current. Analogously to the eq. (21):

$$I = \frac{P_{el}}{V_{bat}} \quad (44)$$

3.6.2 Saturation

The saturation is exploited to limit overcurrent that can leads to a battery overheat and even to cells damage. The saturation limits positive value of current (ex: 300A) during traction request, and the negative value: (ex 100 A) in braking condition.

3.6.3 Thermal model

In this section will be illustrated the block scheme, the thermal model equations applied, and the de-rating control adopted.

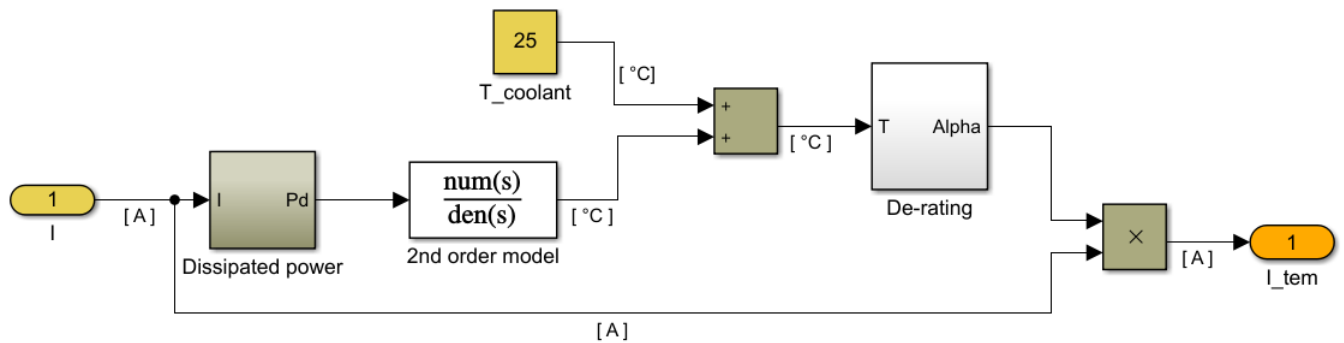


Figure 34: Thermal model.

The first operation is to derive from the current the dissipated power, see eq. (45), then is the turn of the thermal model of 2nd order, which computes the variation of temperature, afterwards is evaluated the battery pack temperature adding the coolant one to the temperature variation, finally a thermal control through a de-rating strategy is applied.

Modelling

[30] The optimal operating temperatures for a lithium ion battery range is from $20\text{ }^{\circ}\text{C}$ to $30\text{ }^{\circ}\text{C}$, however, temperatures between $-40\text{ }^{\circ}\text{C}$ and $60\text{ }^{\circ}\text{C}$ are also allowed. The greater is the cell's working temperature, the higher will be the aging rate. If the temperature becomes excessively high (over $80\text{-}100\text{ }^{\circ}\text{C}$) the active materials inside of the cell may become thermally unstable. On the other hand, at low temperatures, the resistance to lithium ion transport is very high, limiting so electrochemical reactions and therefore the power that can be delivered.

Temperature control is therefore a crucial factor both for performance and battery life. The most widespread thermal model for batteries [31], [30] is the electric circuit model (ECM).

The thermal model developed is showed in the below picture [32], on the left there is represented as power supply the dissipated power, in the upper part are schematized two thermal impedances constituted by:

- R_{th} Thermal resistance
- C_{th} Thermal capacitance

On the right the ambient temperature stands for the coolant temperature, this one will be added to the incremental temperature between the two thermal impedances, obtaining so the final battery pack temperature.

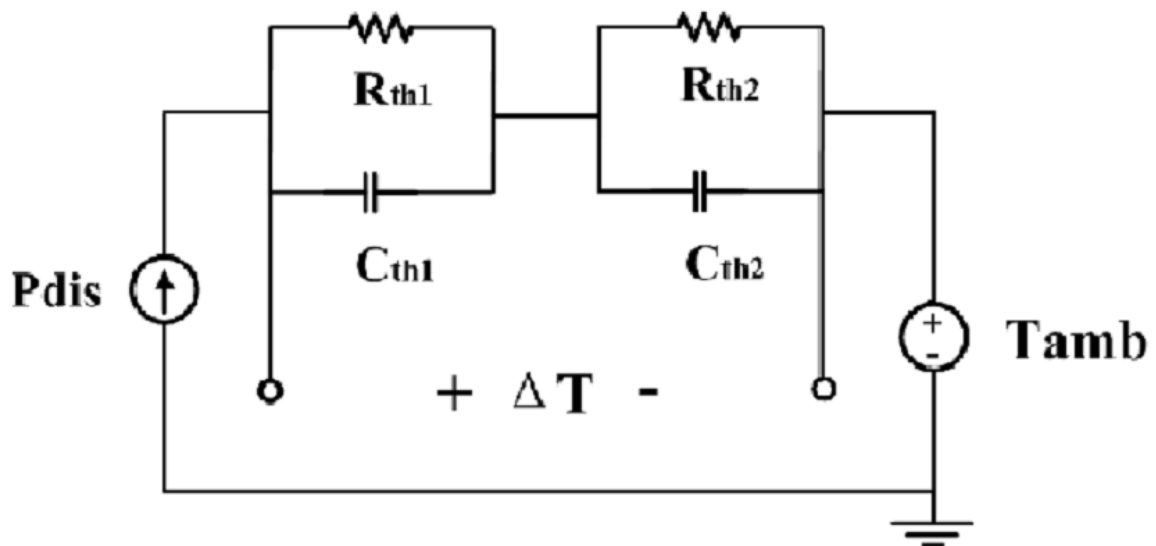


Figure 35: Thermal model of 2nd order.

From the Joule's effect, is known that the dissipated power is:

$$P_{dis} = IR_{eq}^2 \quad (45)$$

Where the resistance R_{eq} is equivalent resistance so derived:

$$R_{eq} = \frac{n_s}{\sum_1^{np} \frac{1}{R_i}} \quad (46)$$

Where:

- n_s is the number of resistances in series.
- n_p is the number of resistances in parallel.
- R is the resistance value

Once the equivalent resistance is known, multiplying it for the square of the instant current, the instant dissipated power is computed, as shown in eq. (45).

At this stage is necessary to introduce the thermal resistance and capacitance values, which are chosen from simulation data.

The analytical scheme of the 2nd order system is the following:

$$\Delta T = P_{dis} \left(\frac{1}{\frac{1}{R_{ch1}} + C_{ch1} \frac{dP_{dis}}{dt}} + \frac{1}{\frac{1}{R_{ch2}} + C_{ch2} \frac{dP_{dis}}{dt}} \right) \quad (47)$$

To solve the system, is introduced the Laplace transform.

Writing the variables in this manner:

- $\Delta T(t) = Y(s)$
- $P_{dis}(t) = X(s)$

Where s represents the Laplace variable, the Transfer Function will be: $G(s) = Y(s)/X(s)$.



Figure 36: Transfer function.

The Transfer function in the Laplace domain is so written:

$$G(s) = \frac{R_1}{1 + \tau_1 s} + \frac{R_2}{1 + \tau_2 s} \quad (48)$$

Where:

- $R_1 = R_{ch1}$ gain of the 1st branch
- $R_2 = R_{ch2}$ gain of the 2nd branch
- $\tau_1 = R_{ch1}C_{ch1}$ transient of the 1st branch
- $\tau_2 = R_{ch2}C_{ch2}$ transient of the 2nd branch

The final shape of the transfer function will be:

$$G(s) = \frac{as + b}{cs^2 + ds + 1} \quad (49)$$

Where:

- $a = R_1\tau_2 + R_2\tau_1$
- $b = R_1 + R_2$
- $c = \tau_1\tau_2$
- $d = \tau_1 + \tau_2$

Exploiting the inverse Laplace transform:

$$g(t) = L^{-1}(G(s))$$

Where:

$$g(t) = \Delta T$$

the final function is converted in time domain, therefore:

$$T = T_{amb} + \Delta T \quad (50)$$

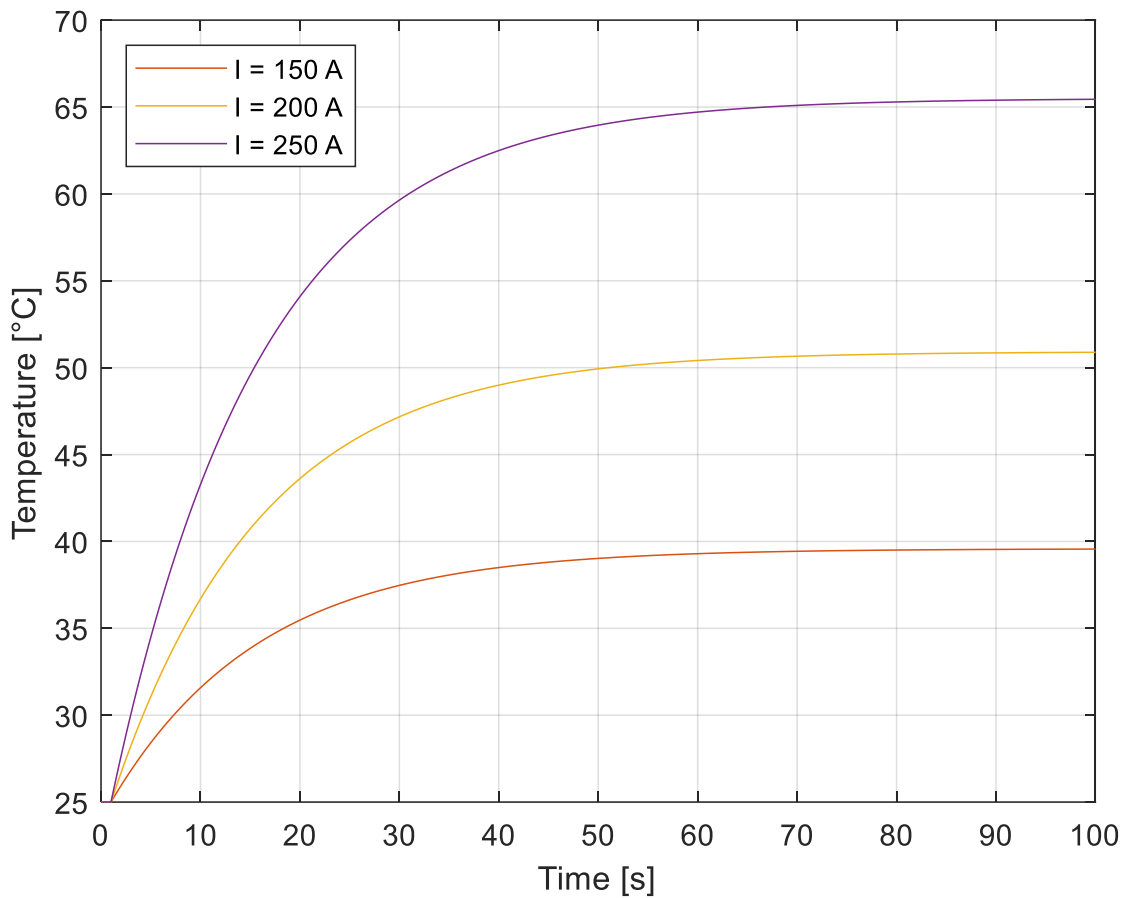


Figure 37: Temperature vs time for different values of current.

De-rating control

To avoid exposing the battery cells at critical temperatures, a saturation control is needed, the working principle is to saturate the current flowing through the cells, reducing so the dissipating power for the highest temperature lowering the temperature, while at low temperature is necessary to interrupt the current to flow avoiding an excess of energy waste due to a high electrochemical resistance.

The control is enabled thanks to a look-up table, see next Figure 38, that for each value of temperatures return a coefficient value that goes from 0 to 1. The current will be multiplied by the coefficient value; therefore, it will be lower than the incoming current if the temperature is lower than 10 °C or higher than 50°C, otherwise it would not vary.

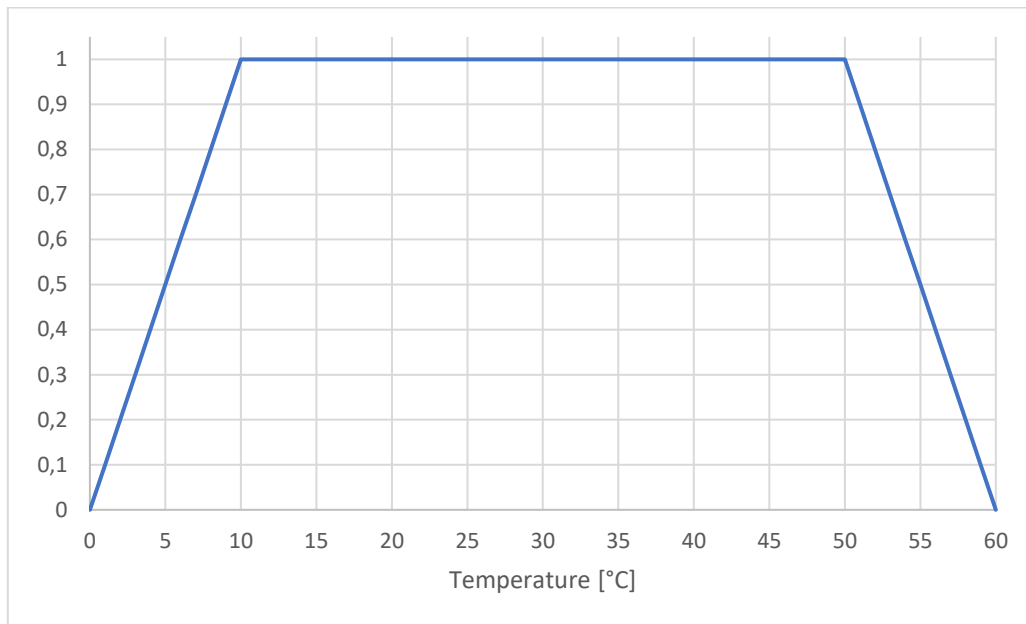


Figure 38: Thermal battery saturation's coefficient.

To summarize and conclude this section, this model receives as input the current and returns the battery pack temperature and the de-rated current.

3.6.4 Battery pack model

This model has in charge to represent the cells layout and their characteristics, which is described by the open circuit voltage curve vs depth of discharge, see Figure 41.

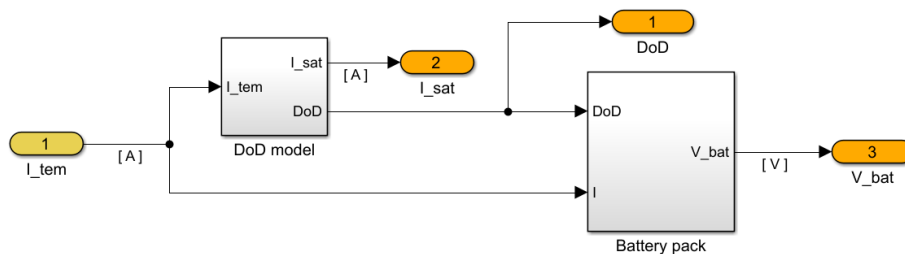


Figure 39: Cell model.

The input is the current coming from the thermal model, while the outputs are the battery voltage, the saturated current, and the battery depth of discharge.

DOD model

The first step of this model is to evaluate the depth of discharge, the calculation is based on the following equation:

$$DoD [\%] = DoD_0 + \frac{100}{3600C} \int i dt \quad (51)$$

Where:

- DoD_0 [%] is the depth of discharge of the battery at time 0
- i [A] is the current
- C [Ah] is the battery capacity, so evaluated:

$$C = n_p C \quad (52)$$

Where:

- n_p is the number of cells in parallel
- C [Ah] is the cell capacity

The DoD value will be used in the next block to derive the open circuit voltage of the cells; furthermore, the current will be saturated when the DoD reach the value of 100 %.

Battery pack

In this section will be discussed the development of the battery pack model.

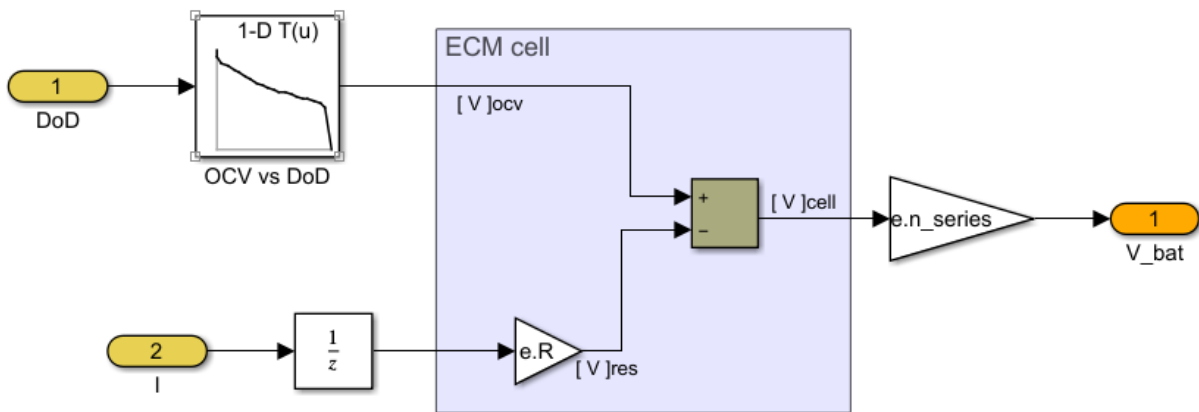


Figure 40: Battery pack block.

The first input is the value of the depth of discharge, it enters in the look-up table with the cell open circuit voltage (OCV) vs DoD values.

OCV vs DoD characteristic

Every battery has a voltage values that has a maximum peak when it is fully charged and slowly decreases till its minimum value when it is completely discharged.

The voltage value is called Open Circuit Voltage OCV, every cell is described by a discharging curve characteristic.

The cell taken in exam has the following open circuit voltage behavior:

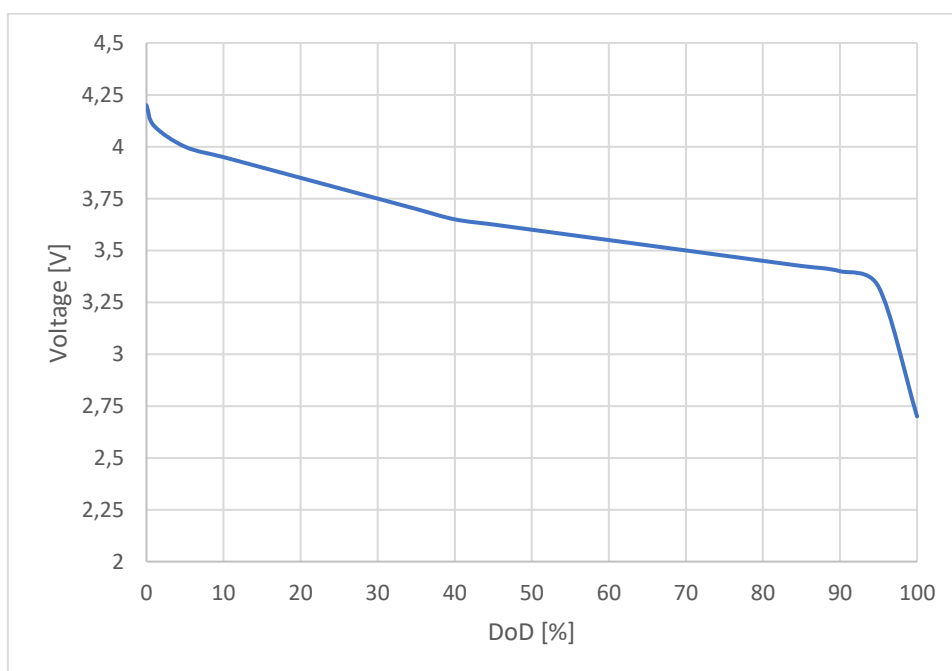


Figure 41: OCV vs DoD.

Is it clear to note that when the cell is fully charged has a voltage of 4.2 V, then steeply decreases to 4.0 V for a depth of discharge of about 5 %, then in a range of 5 % to 95 % the OCV has a linear characteristic that will bring the voltage from 4.0 V to 3.4 V. Finally, the OCV drops to 2.7 V for DoD that are approaching the 100 % value.

The second output is the current, together with the open circuit voltage value and the cell internal resistance, creates the electric circuit model of the cell, schematized below:

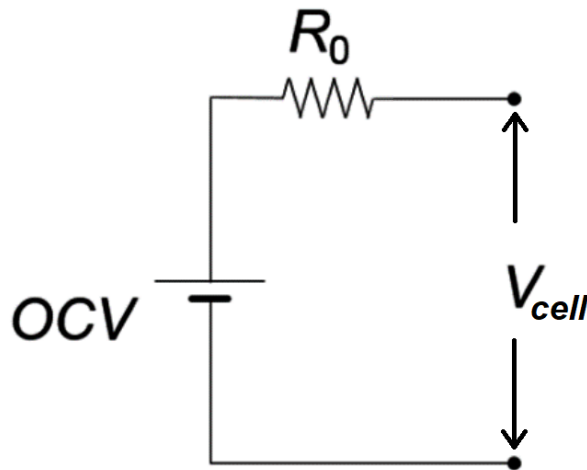


Figure 42: Electric circuit model of the cell.

The internal resistance is gathered from the technical data and is considered as a constant, since the cell configuration can be of parallel type the internal resistance R_0 is so computed:

$$R_0 = \frac{R}{n_p} \quad (53)$$

Where:

- R is the internal resistance of the cell,
- n_p is the number of cells in parallel.

Therefore, the cell in parallel voltage, can be so derived:

$$V_{cell} = OCV - R_0 I \quad (54)$$

To conclude, the battery pack voltage is evaluated, multiplying the cell in parallel voltage times the total number of cells in series:

$$V_{bat} = n_s V_{cell} \quad (55)$$

3.6.5 Outputs

The ending part of this model is composed of the system outputs, the first output is the depth of discharge computed by the battery pack model. The second output is the battery power, calculated starting from the battery pack outputs: saturation current and battery voltage, exploiting the electric power definition:

$$P_{bat} [W] = V_{bat} I_{sat} \quad (56)$$

The battery power is needed also to compute the battery energy consumption, thanks to the following formula:

$$E [kWh] = \frac{1}{3.6 * 10^{-6}} \int P_{bat} dt \quad (57)$$

The energy value is useful to evaluate the effectiveness of the regenerative braking, it is reachable simply evaluating the difference, in terms of energy consumption, of one driving cycle with and without the limit on the negative current.

To conclude, the last output is the state of charge, that is complementary to the depth of discharge parameter:

$$SoC [\%] = 100 - DoD$$

(58)

While the depth of discharge starts from 0% when the battery is fully charged and reach the value of 100% when is fully discharged, the state of charge does the opposite, it signals 0% for an empty battery and 100% for a fully charged one.

4 MODEL VALIDATION

To support and validate the thesis work has been chosen an electric vehicle with known technical data and performance, the vehicle chosen is the Renault Zoe.



Figure 43: Renault Zoe.

Most of the information needed to develop the model were available in the next table, some of them has been retrieved from different sources:

Engine map efficiencies: from internal data of a similar motor

The motor inertia: from a similar motor [33]

Wheel Inertia: from an appendix of the book: [17].

Rolling resistance coefficients: Class C pneumatic reference.

Transmission efficiency: from similar drivetrain [33]

Cell data: Kokam pouch cell, see Table 1, with the cell capacity changed to fit the battery available energy, see Table 3

Table 2: Renault Zoe technical data.



RENAULT ZOE TECHNICAL SPECIFICATIONS

	ZOE Q210	ZOE R240
PERFORMANCE		
Motor type	5Agen2	5Agen3
Technology	100 % electric – Synchronous electric motor rotor coil	
Max Power kW CEE (ch)	65 (88)	
Max Power at (rpm)	3,000 to 11,300	
Max Torque Nm CEE (Nm)	220	
Max torque at (rpm)	250 to 2,500	
Maximum speed (km/h)	135	
0 - 50 km/h (s)	4	
0 - 80 km/h (s)	8,6	
0 - 100 km/h (s)	13.5	
Gearbox	Gear reduction	
Number of gears	1	
BATTERY		
Technology	Lithium-ion	
Total voltage (Volts)	400	
Number of modules	12	
Number of cells	192	
Available energy (kWh)	22	
Weight (Kg)	290	
CHARGE		
Charger	Adaptive, single or three-phase, between 2 and 43W	
Green-Up reinforced socket	10 hrs	9 hrs
3 kW (16A single phase wallbox)	9 hrs	Less than 8 hrs
7 kW	4 hrs	
22 kW (32A three-phase station)	80% in 1 hr	
43 kW (63A three-phase station)	80% in 30 min	80% in 1 hr
CONSUMPTION		
Range NEDC (km)	210	240
Range: suburban driving	100/150	115/170
CO2 emission at use (g/km)	0	
STEERING		
Power steering	Yes (electric)	
Turning circle between kerbs/ walls (m)	10.56	
Number of turns of steering wheel	2.73	
AXLES		
Front	Pseudo Mac-Pherson	
Rear	Torsion beam	
Anti-roll bar ø front / rear (mm)	23/25	
TYRES AND WHEELS		
Reference wheels (")	15" (Life) 16" (Zen and Intens)	
Tyre dimensions	Michelin ENERGY low consumption – 185/65 R15 – 195/65 R16	
BRAKING		
ABS	Yes	
Emergency brake assist	Yes	
Electronic brake distribution	Yes	
ESC	Yes	
Front disk : type (and size in mm)	Ventilated disk (258)	
Rear disk : type and Ø (mm)	Drums 9"	
Parking brake	Manual	
AERODYNAMICS		
SCx	0.75	
WEIGHT (Kg)		
Kerb weight	1,468	
Kerb weight on the front	871	
Kerb weight on the rear	597	
Gross Train Weight (M.M.A.C.)	1,943	
Within the limit of M.M.A.C. max.	1,023 on the front / 920 on the rear	

As visible in the Table 2, for the Renault Zoe are available several technical data, the used are listed below.

Vehicle data

- Vehicle mass
- Aerodynamics
- Mass distribution F/R

Powertrain data

- Motor characteristics:
 - Max power
 - Rpm range with max power
 - Max torque
 - Rpm range with max torque

Wheel data

- Tire dimensions

Battery data

- Technology
- Number of cells
- Available energy

The data, instead, exploited to validate the model are:

Performance

- 0-50 km/h (s)
- 0-80 km/h (s)
- 0-100 km/h (s)

Range

- NEDC range

Battery

- Available energy
- Weight

In the next paragraph will be illustrated the results of the model starting with the forward approach model, to conclude with the backward approach one.

Motor

Derived from abovementioned technical data:

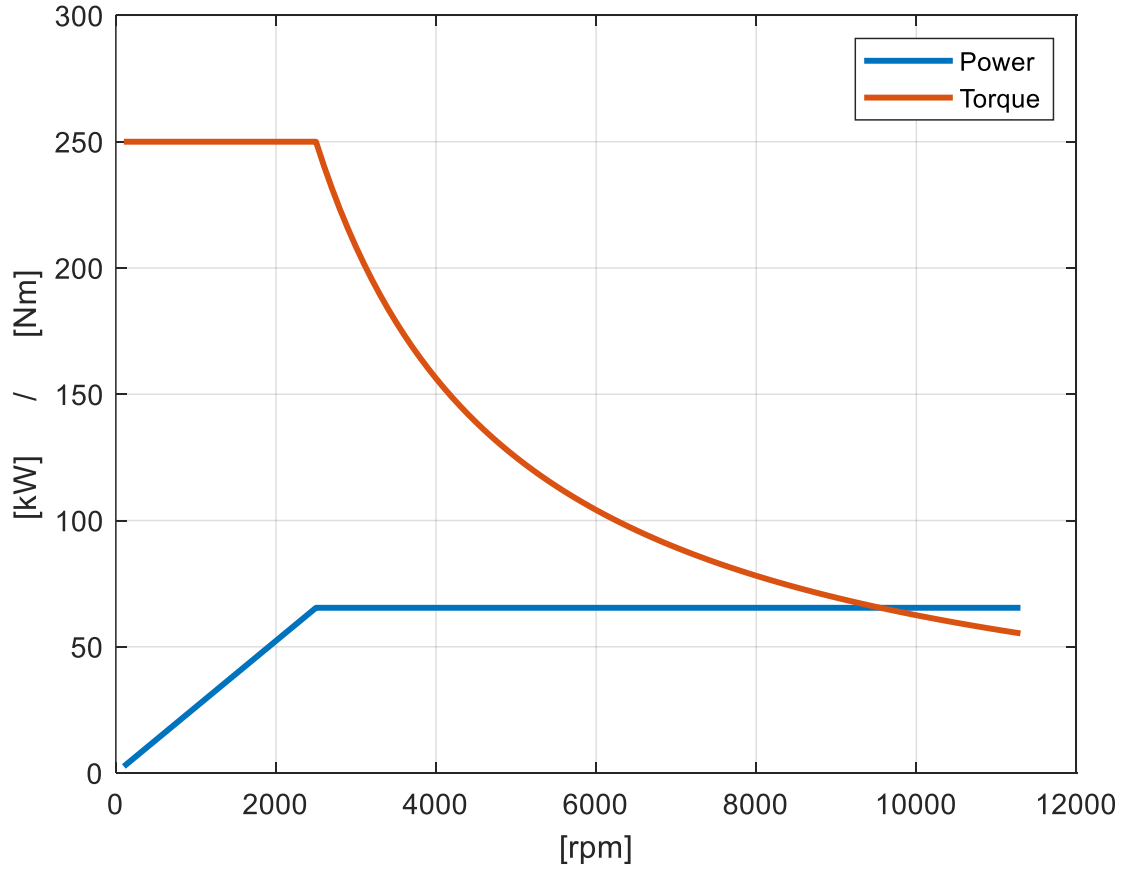


Figure 44: Zoe motor electric power Torque map

Cell input:

Table 3: Kokam pouch cell modified data.

Nominal voltage	3.7	V
Capacity	34.5	Ah
$c - rate_{nom}$	5	
$c - rate_{peak}$	8	
Weight	1080	g
Internal resistance	0.009	Ohm

4.1 FORWARD APPROACH MODEL RESULTS

Performance

- 0-50 km/h: 3,72 s
- 0-80 km/h: 8,28 s
- 0-100 km/h: 13,48 s

Battery

- n° series = 96
- n° parallel = 2
- Battery energy = 25,9 kWh
- Available battery energy = 22 kWh (85%)
- Weight = 207 kg
- Pack weight = 280 kg

Range

- NEDC: 205 km
- WLTP: 167 km

The main result of the forward model is the battery pack model, below is showed a table with the model results on the left side and the Zoe technical data on the right side.

Table 4: Battery results comparison.

Parameters	Model results	Zoe battery pack data	variation
n° cells	192	192	0%
n° cells in parallel	2	-	-
n° cells in series	96	-	-
Total energy [kWh]	24.5	-	-
Available energy [kWh]	22	22	0%
Battery pack weight [kg]	280	290	-3.5%

The table clearly shows as the battery pack results can be assumed affordable in predicting or verifying the battery pack design.

4.2 BACKWARD MODEL RESULTS

Performance

Table 5: Performance comparison.

speed / mux	0,8	0,85	0,9	0,95	1	Zoe	Δ
0-50	4,4	4,25	4,1	3,95	3,8	4	-6.25%
0-80	8,7	8,5	8,3	8,2	8	8,6	-1%
0-100	13,1	13	12,8	12,65	12,55	13,5	-3.7%
0-135	26,9	26,8	26,6	26,5	26,35	-	-

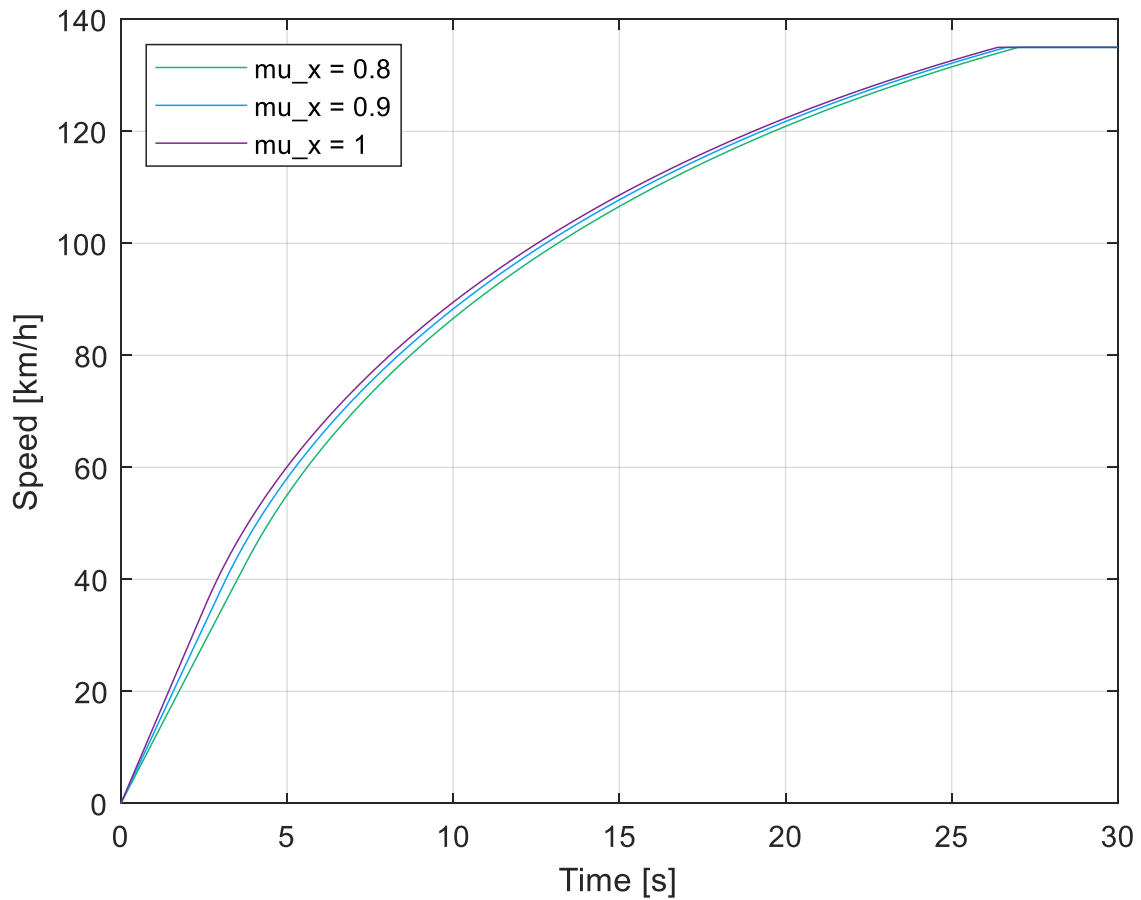


Figure 45: Renault Zoe evaluated performance.

As showed in the above Table 5, and Figure 45: Renault Zoe evaluated performance., the performance curve are obtained for several values of the static coefficient of friction μ_x , the results are quiet accurate, especially for $\mu_x = 0.85$.

In the specific the most accurate value, independently from the chose friction coefficient is the time to reach 0-80 km/h.

Range

Table 6: Range comparison

Cycle	Range [km]	Zoe range [km]
NEDC	217,4	210-240
WLTC	175,6	-

The range results are validated by the data provided about NEDC range, as visible in the above table, there are two values for the NEDC range, one is achieved with an electric motor of first generation, the other one with a new generation motor. Since the efficiency motor of both the electric motor are not retrievable, an in-house map was used, therefore a higher accuracy is not possible to achieve with the available information.

5 CASE STUDY

After the thesis work validation, the longitudinal dynamic model is exploited to predict the performance and the range behavior of an electric vehicle in development. Moreover, some battery parameters as current, state of charge and temperature are plotted, since are useful to calibrate the battery management system of the vehicle in development.

The electric vehicle considered belongs to the b segment with rear wheel drive, the main technical data are listed below.

Vehicle data

- Curb mass: $m = 1380 \text{ kg}$
- Mass distribution F/R: 45/55 %
- Aerodynamic coefficient: $SC_x = 0.732 \text{ m}^2$
- Wheelbase: $l = 2580 \text{ mm}$
- Height of the center of mass $h_g = 450 \text{ mm}$

Powertrain data

- Motor inertia: $J_m = 0.06 \text{ kgm}^2$
- Transmission ratio: $i = 9.59$
- Transmission efficiency: 0.97

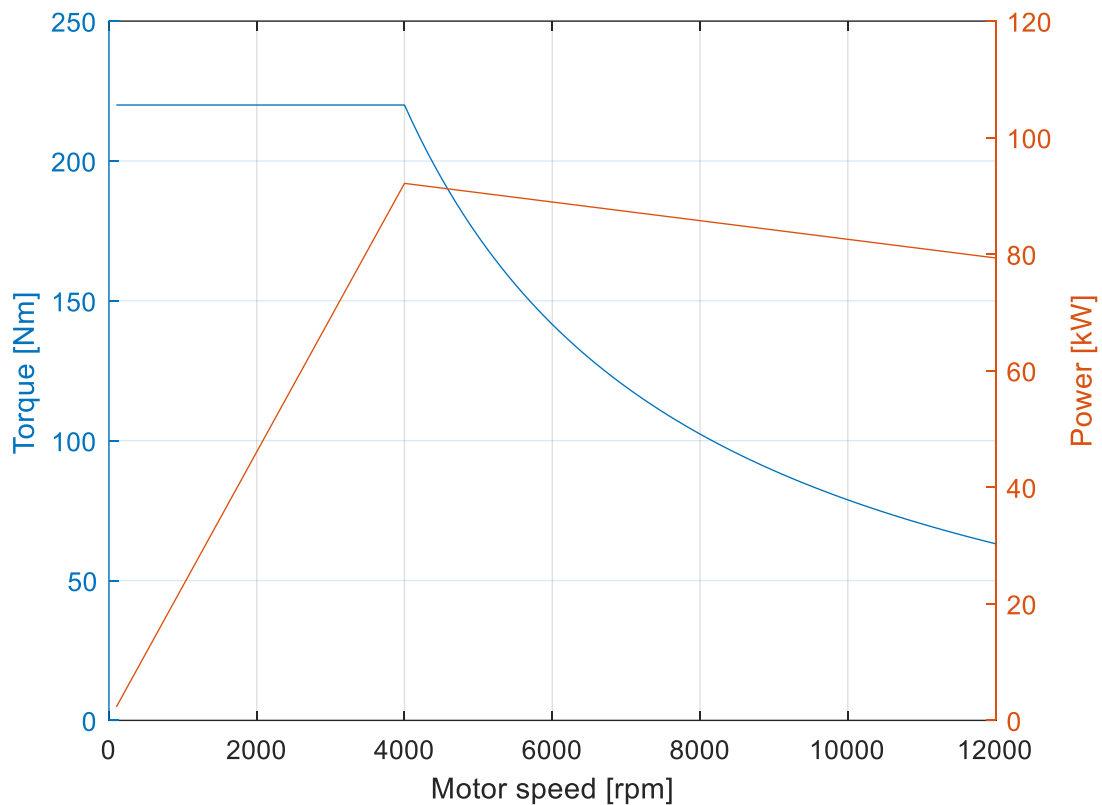


Figure 46: CS Motor map.

Tire data

- 155/70 R19
- Wheel inertia: $J_w = 0.6 \text{ kgm}^2$
- Static friction coefficient: $f_0 = 0.0084$
- Dynamic friction coefficient: $k = 6.5 \cdot 10^{-6} \text{ s}^2/\text{m}^2$

Battery data

- Cell: see Table 1
- Battery pack:

Table 7: CS Battery pack configuration.

n° cells	216
n° cells in parallel	2
n° cells in series	108
Total nominal voltage	400 V
Total energy	42.4 kWh

5.1 PERFORMANCE AND RANGE RESULTS:

The expected performance and the vehicle range with the standard driving cycle NEDC and WLTC are summarized in the below table and shown graphically in the following pictures.

Performance	
0-40 km/h	3.0 s
0-80 km/h	6.5 s
0-100 km/h	9.4 s
0-160 km/h	31.0 s
Range	
NEDC	338.1 km
WLTC	272.0 km

Performance

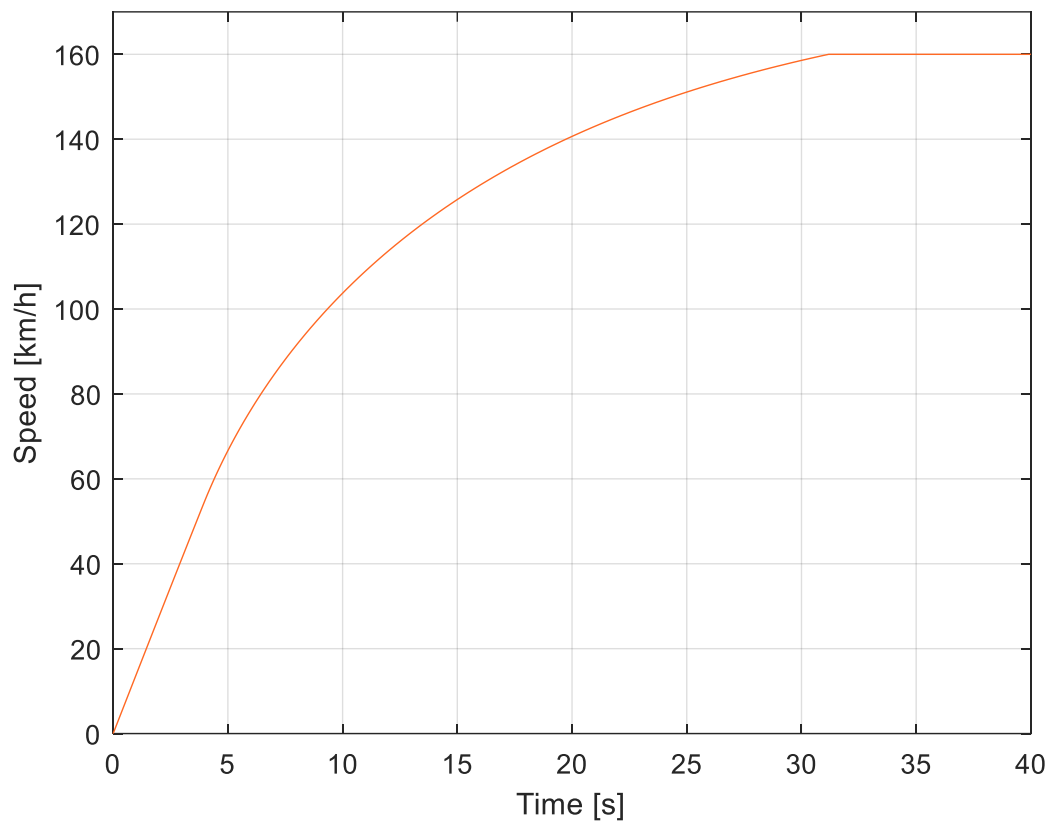


Figure 47: CS Performance.

In the next pages are illustrated the vehicle range for NEDC and WLTC cycles, is worth to note that the motor torque is stopped when a value of 15% of state of charge is reached, this limit is imposed to preserve the battery capacity during its lifecycle.

5.1.1 NEDC range

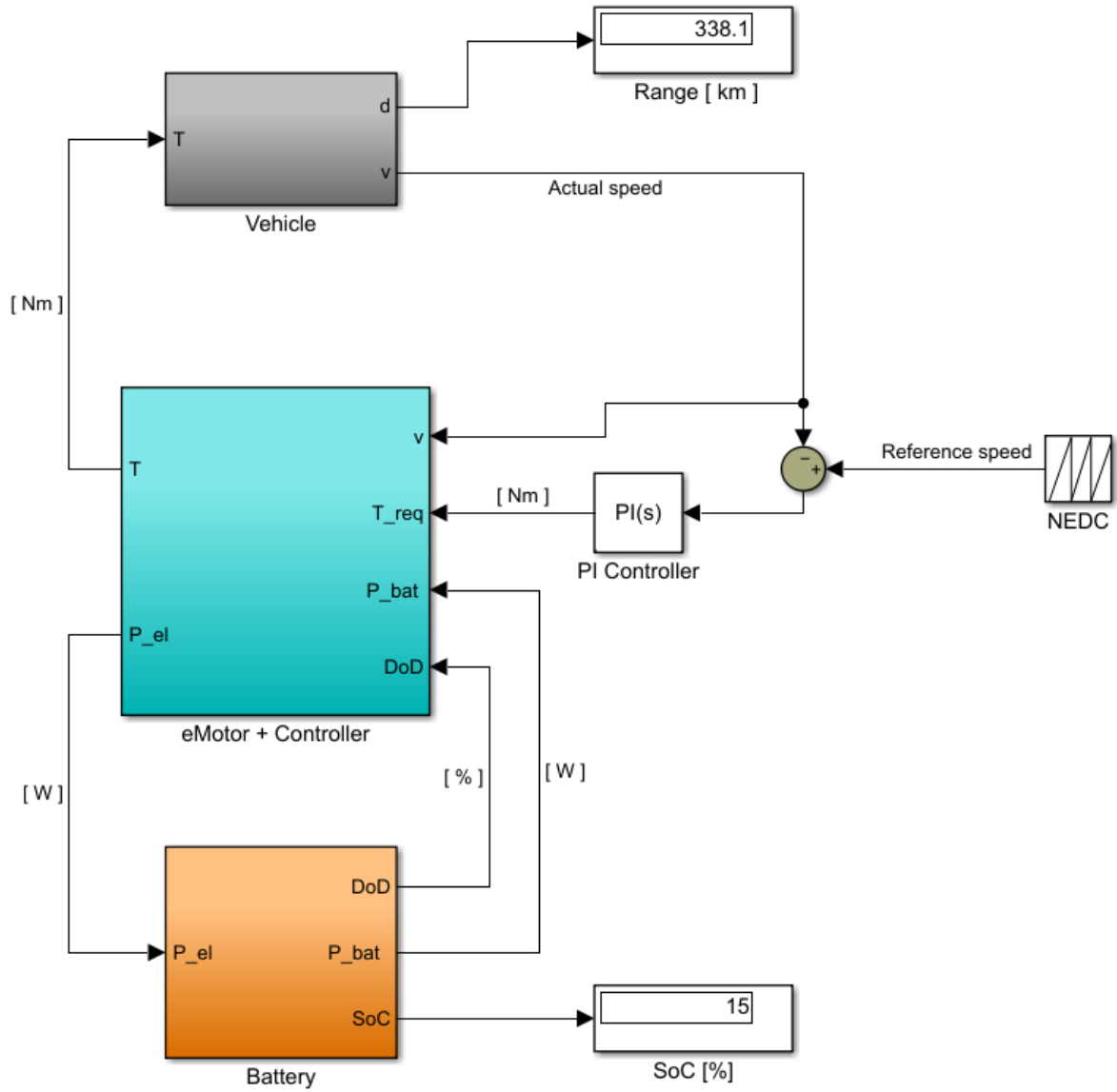


Figure 48: CS NEDC range.

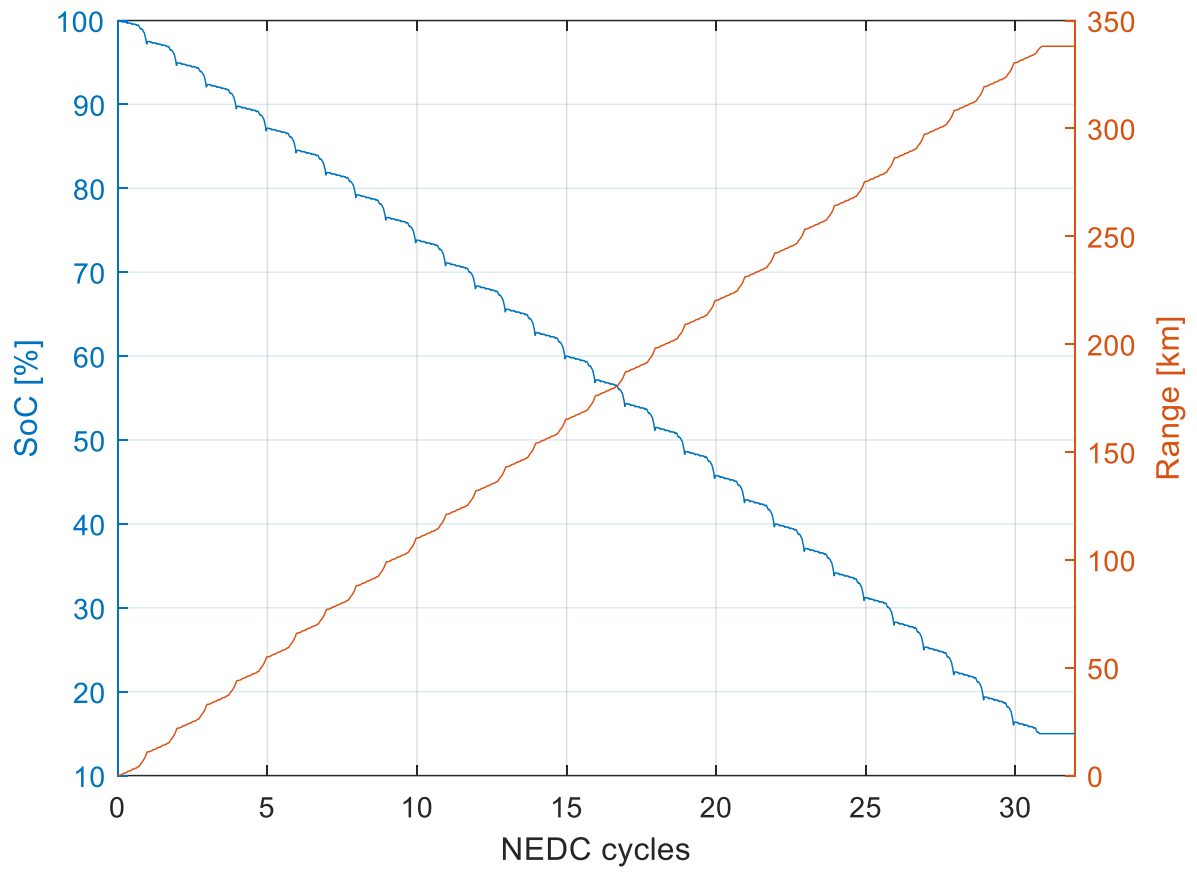


Figure 49: CS NEDC range and SoC.

5.1.2 WLTC range

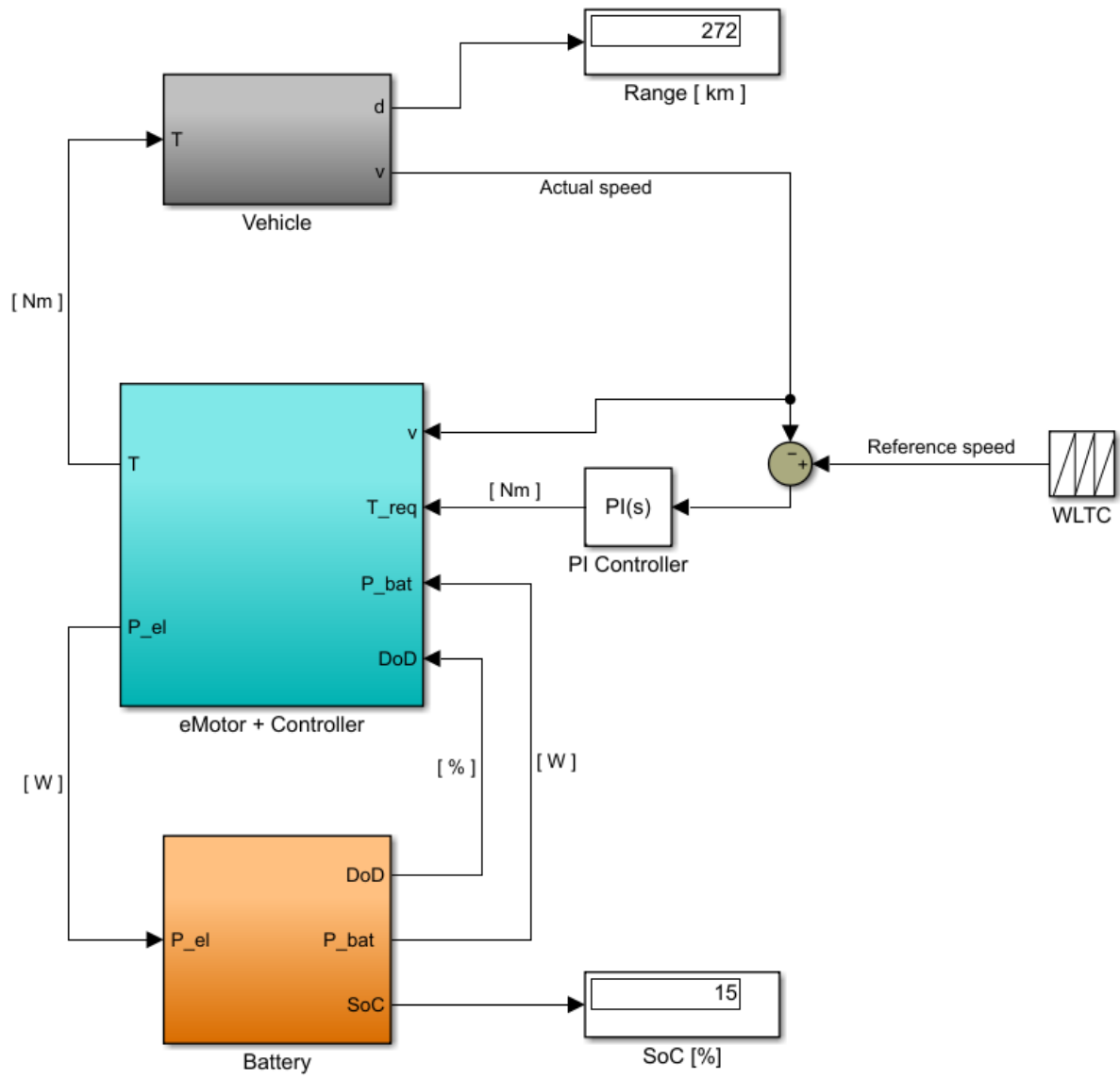


Figure 50: CS WLTC range.

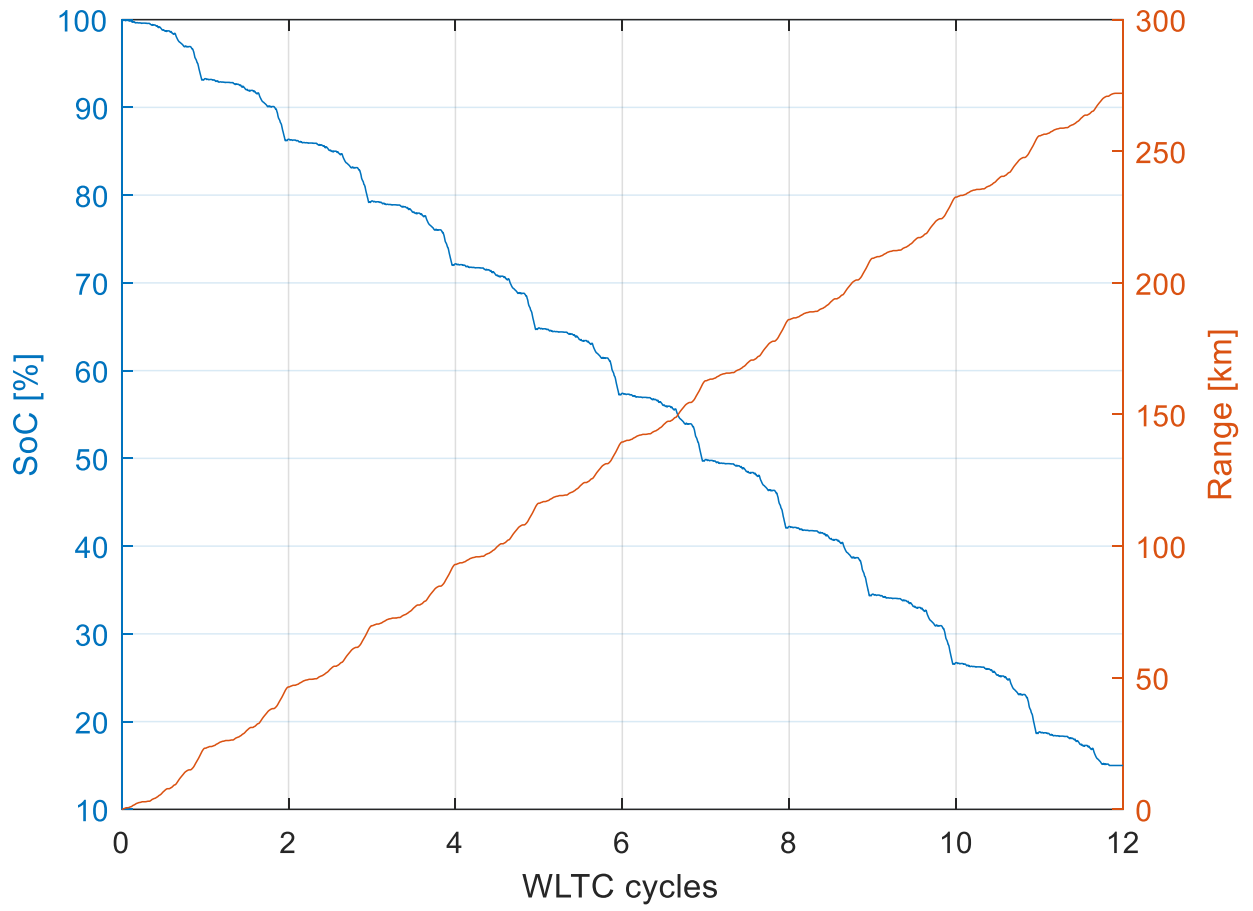


Figure 51: CS WLTC range and SoC.

5.2 BATTERY PARAMETERS

In this section will be showed a specific speed cycle with severe acceleration so that the current behavior either in traction and in regenerative braking is showed.

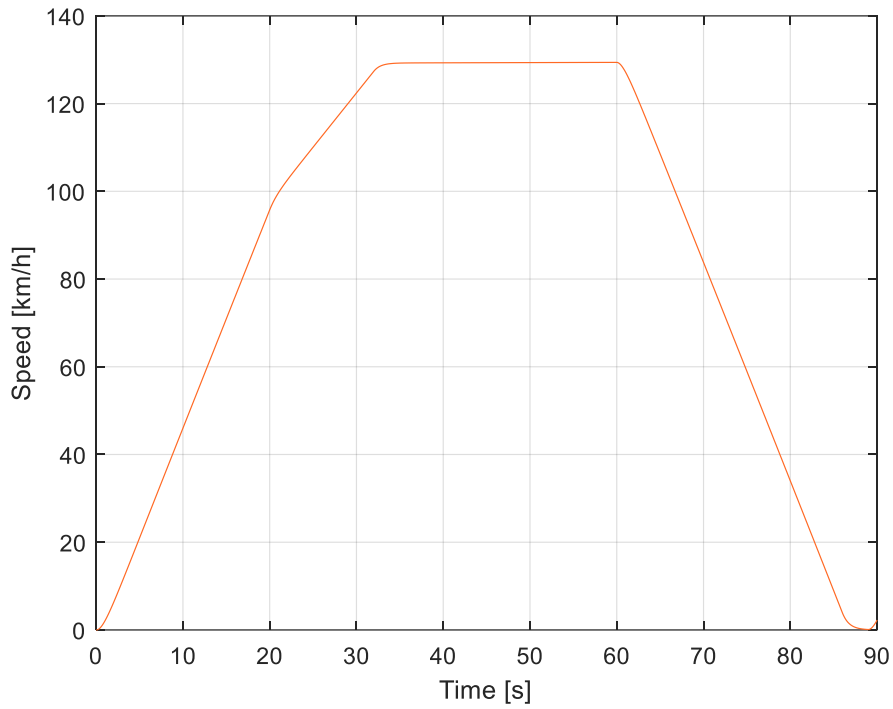


Figure 52: CS reference cycle.

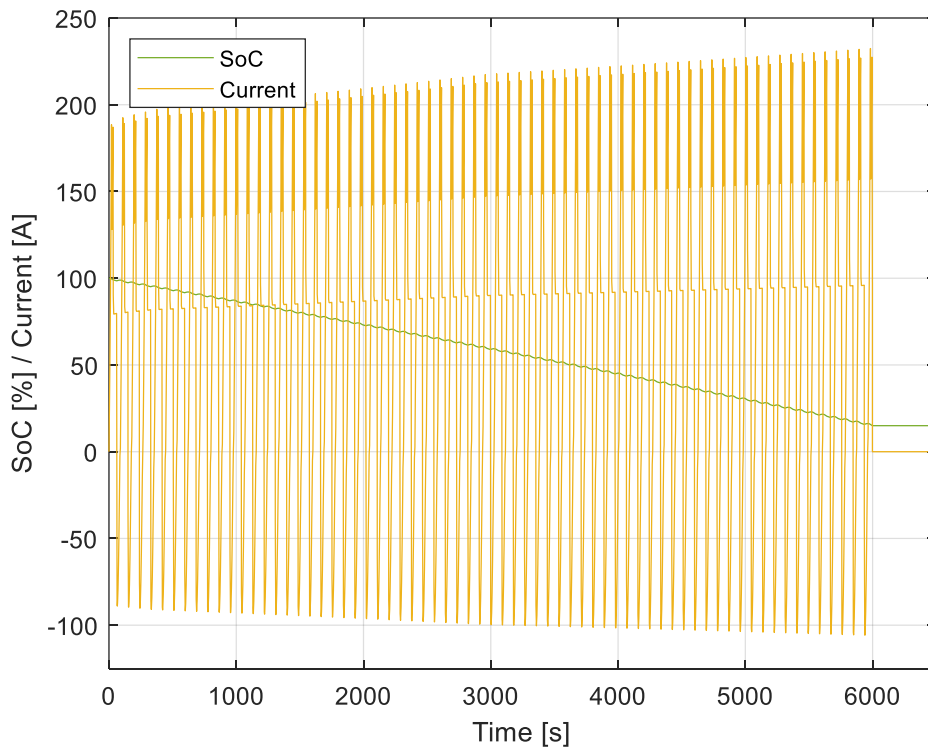


Figure 53: CS SoC and Current for Repeated reference cycle

5.3 REGENERATIVE BRAKING

The aim of this paragraph is to show how to change some parameters directly on Simulink, in the specific will be illustrated how to set the limit on the negative current, in order to regulate the amount of regenerative braking.

Opening the saturation block inside the battery block, see Figure 31: Battery block from outside., will be displayed the following window:

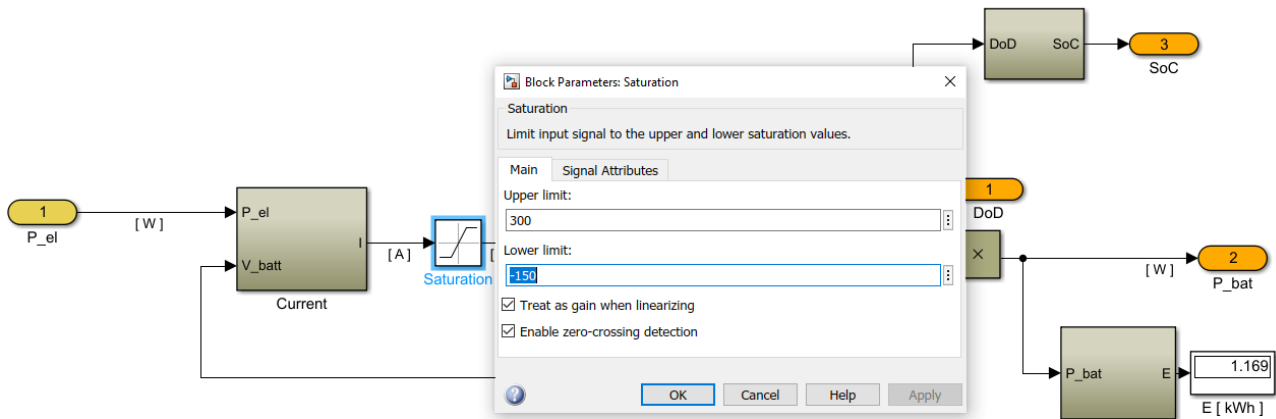


Figure 54: Simulink - Regenerative braking.

In the upper picture is showed an example of 1 NEDC cycle ran, with a regenerative current limit set to -150 A and a consequent energy consumption of 1.169 kWh.

If the negative current limit is set to 0 A, the energy consumption will raise to 1.51 kWh, as shown in the below figure:

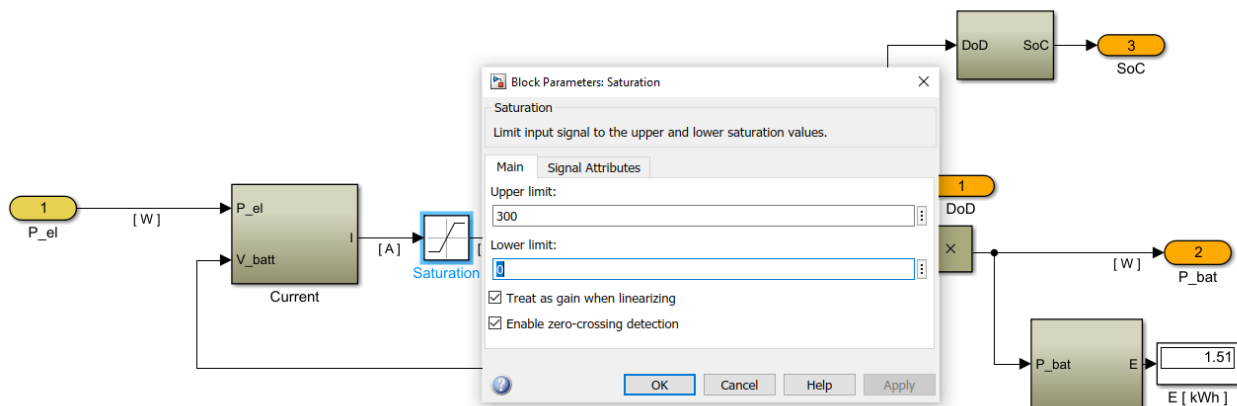


Figure 55: Simulink - No regenerative braking.

This simulation is interesting because shows how much energy can be saved thanks to the regenerative braking, in the next table will be collected the difference in terms of energy consumption of using or not a regenerative braking.

Table 8: Energy comparison.

Cycle	Reg. Braking	No Reg. Braking	Variation
NEDC [Wh]	1169	1510	+29 %
WLTC [Wh]	3094	3882	+25 %

5.3.1 Total range comparison

In this section is compared the total vehicle range with the driving cycles with the regenerative braking and without it.

NEDC

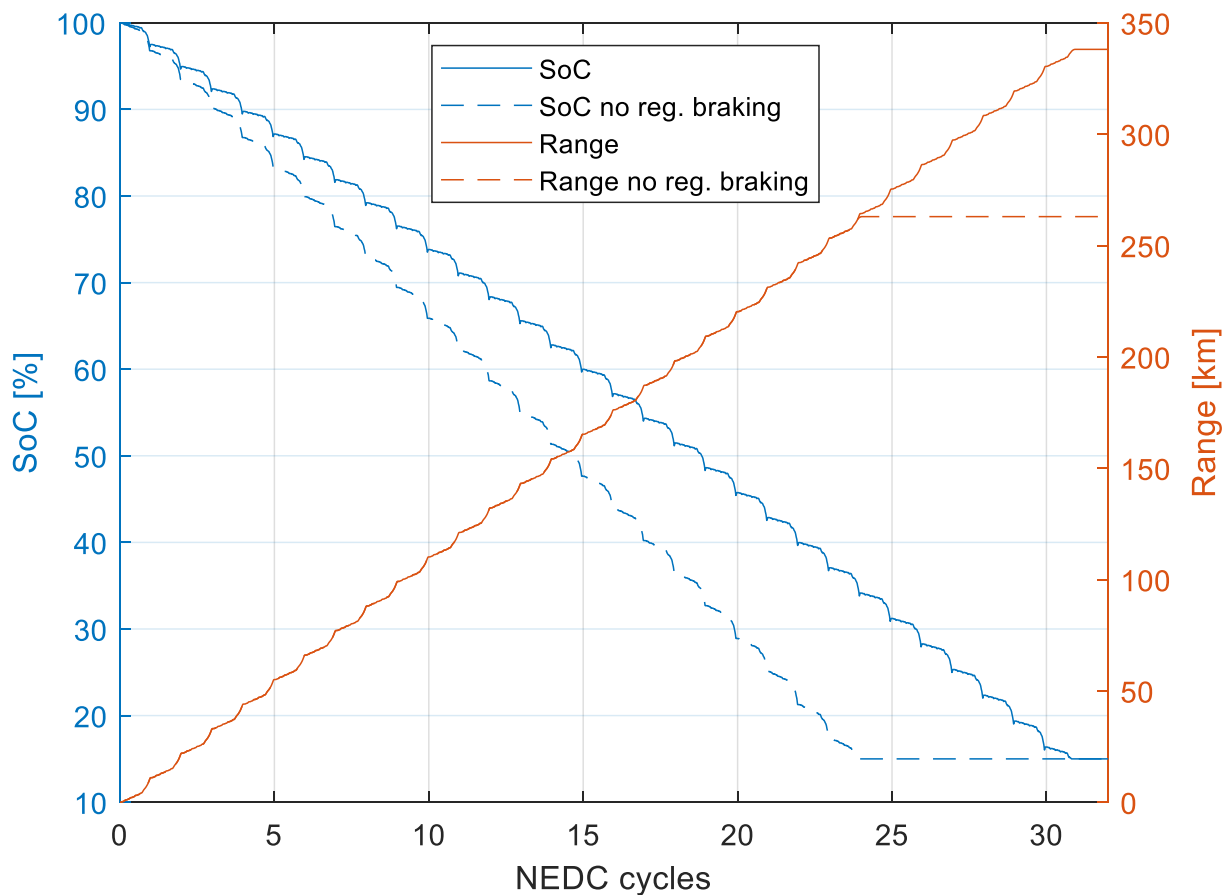


Figure 56 :CS NEDC range with and without regenerative braking.

WLTC

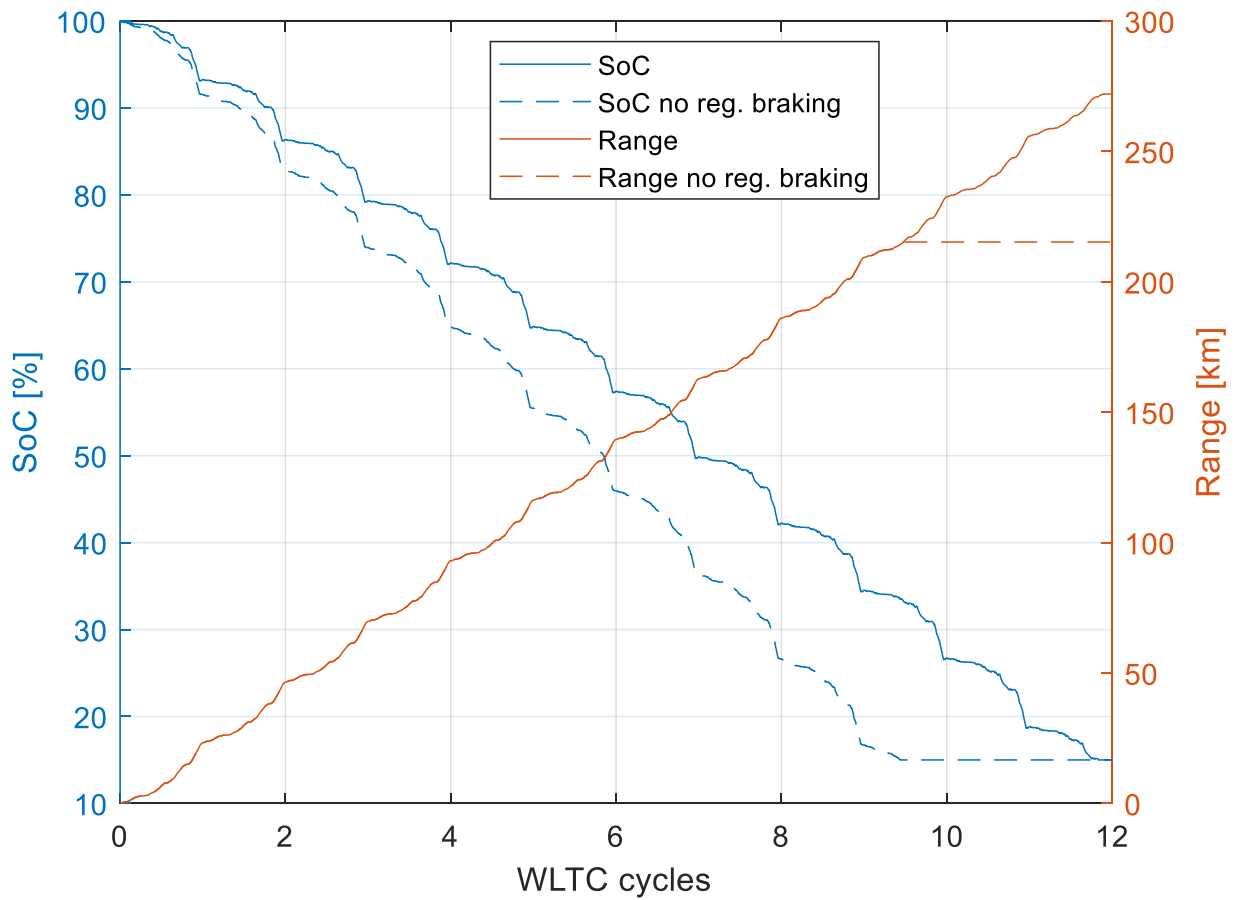


Figure 57: CS WLTC range with and without regenerative braking.

In the below table are summarized the range values of both the standard cycles, highlighting the regenerative braking impact and the range.

Table 9: Range comparison.

Cycle	Reg. Braking (-150 A)	No Reg. Braking	Variation
NEDC [km]	338.1	263	+28.5 %
WLTC [km]	272	215.3	+26.3%

The results show that the regenerative braking allows an extension of range of more than 25 % respect the case with no regenerative braking, that is an interesting value, knowing that the range is represents one of the weakest points of the electric mobility.

5.4 THERMAL BATTERY MANAGEMENT

The model is equipped with a thermal management control, in the below picture is illustrated how the intervention of the de-rating control, during a performance cycle, prevent the battery pack to reach temperature above 60°C.

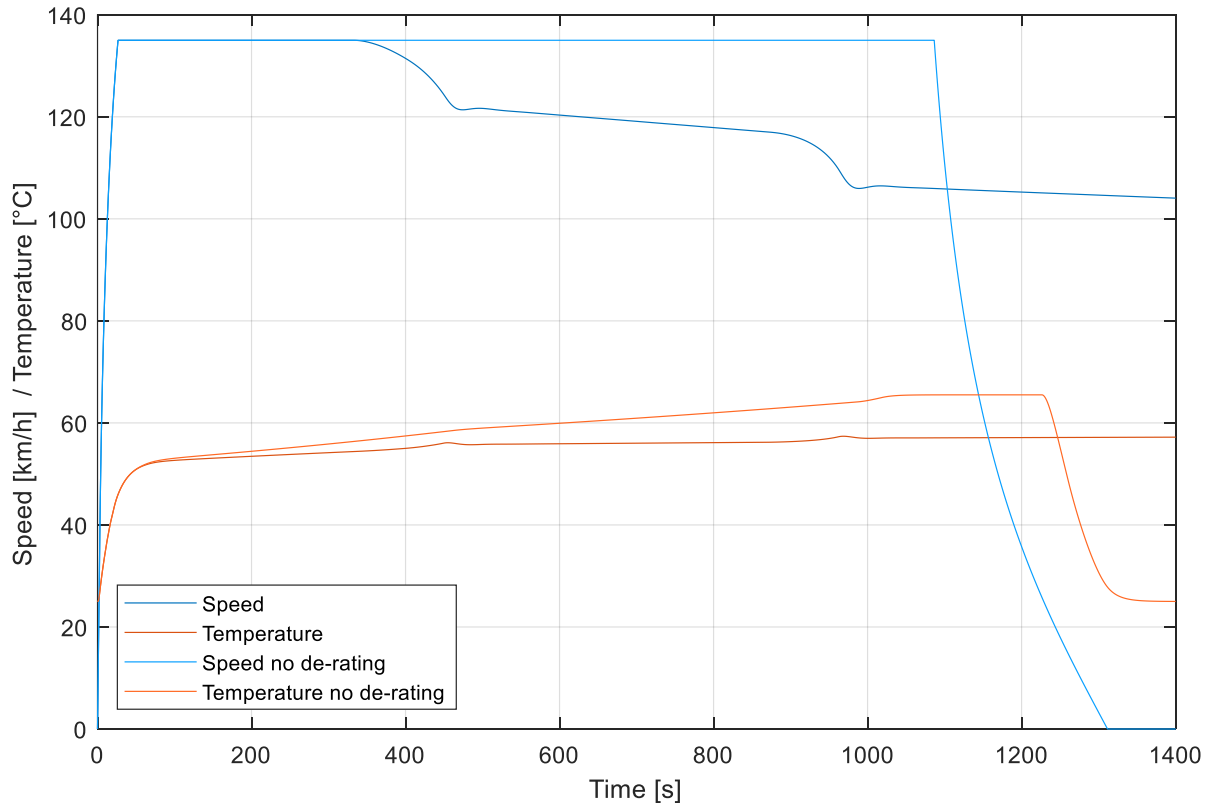


Figure 58: CS temperature and speed.

6 USER GUIDE

In this last chapter will be showed how to use the backward approach model to retrieve the desired outputs.

The user guide is divided in two paragraphs, the first one concerns the input insertion using the Matlab model, while the second one is about the result visualization developed on Simulink.

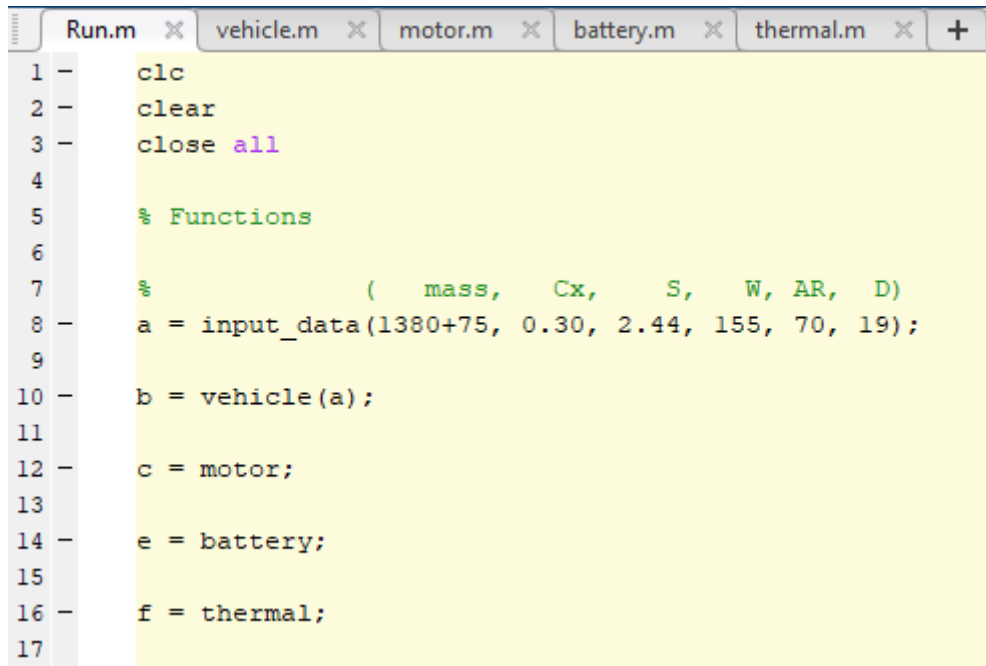
6.1 MATLAB

The editor page of the model is exploited to insert the main vehicle and tire inputs and to initializes the other pages containing functions with different inputs, grouped by their common properties.

All the most important Matlab files will be showed and explained below.

6.1.1 Run

This page is the editor one, used to initialize all the input of the model.



```
Run.m x vehicle.m x motor.m x battery.m x thermal.m x +
1 -   clc
2 -   clear
3 -   close all
4
5   % Functions
6
7   %           ( mass, Cx, S, W, AR, D)
8 -   a = input_data(1380+75, 0.30, 2.44, 155, 70, 19);
9
10 -  b = vehicle(a);
11
12 -  c = motor;
13
14 -  e = battery;
15
16 -  f = thermal;
17
```

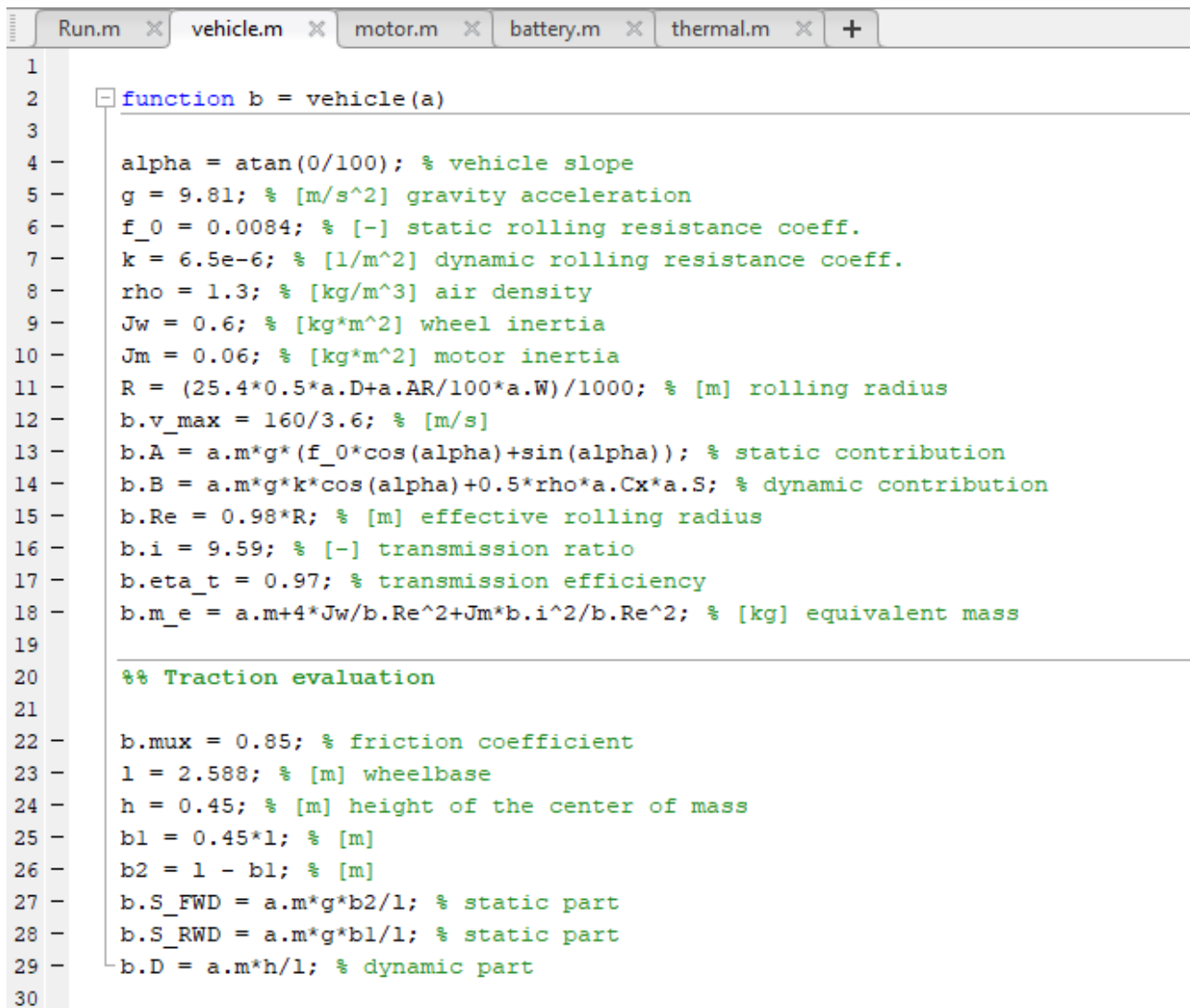
Figure 59: Matlab - Run.

In addition to the editor functions, this page loads the workspace with the following input data:

- Vehicle mass
- Drag coefficient
- Transversal surface
- Tire width
- Tire aspect ratio
- Wheel diameter

6.1.2 Vehicle

This Matlab function collects data and computes preliminary calculus needed for the vehicle block in Simulink model, see paragraph 3.3.

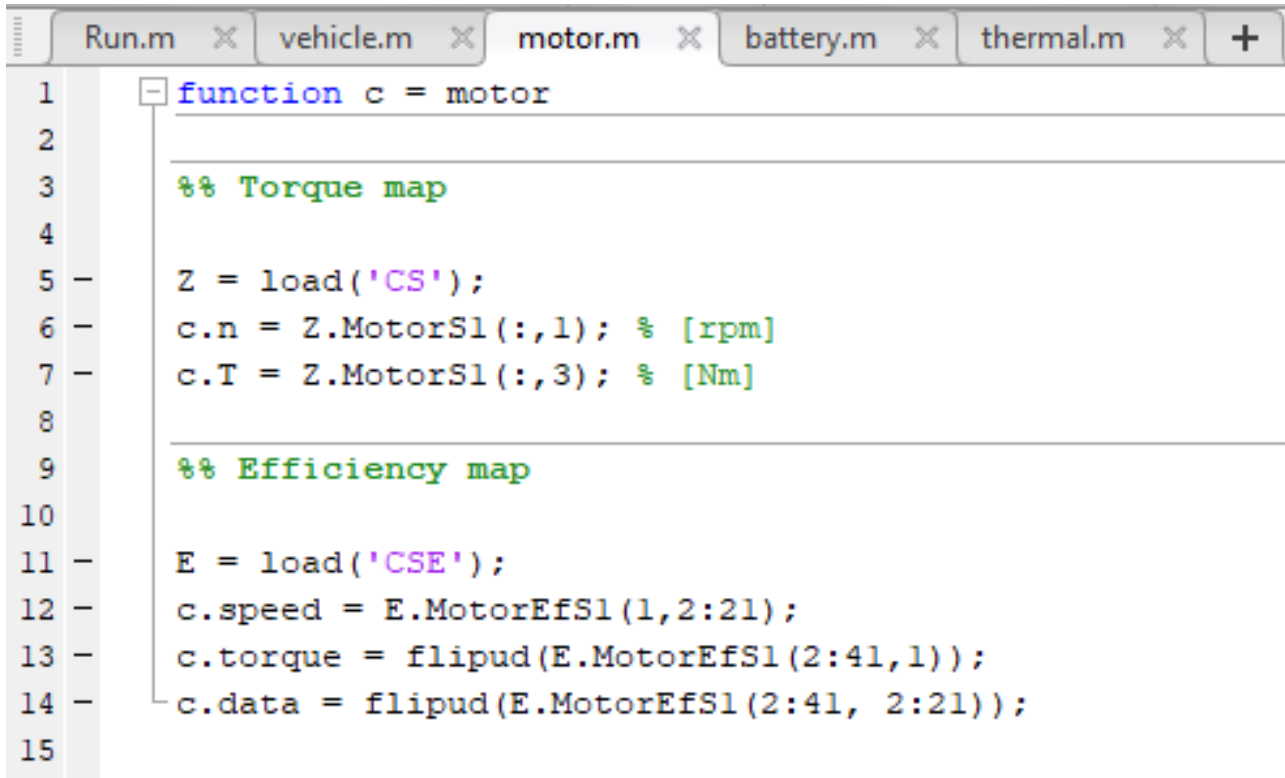


```
1
2 function b = vehicle(a)
3
4 alpha = atan(0/100); % vehicle slope
5 g = 9.81; % [m/s^2] gravity acceleration
6 f_0 = 0.0084; % [-] static rolling resistance coeff.
7 k = 6.5e-6; % [1/m^2] dynamic rolling resistance coeff.
8 rho = 1.3; % [kg/m^3] air density
9 Jw = 0.6; % [kg*m^2] wheel inertia
10 Jm = 0.06; % [kg*m^2] motor inertia
11 R = (25.4*0.5*a.D+a.AR/100*a.W)/1000; % [m] rolling radius
12 b.v_max = 160/3.6; % [m/s]
13 b.A = a.m*g*(f_0*cos(alpha)+sin(alpha)); % static contribution
14 b.B = a.m*g*k*cos(alpha)+0.5*rho*a.Cx*a.S; % dynamic contribution
15 b.Re = 0.98*R; % [m] effective rolling radius
16 b.i = 9.59; % [-] transmission ratio
17 b.eta_t = 0.97; % transmission efficiency
18 b.m_e = a.m+4*Jw/b.Re^2+Jm*b.i^2/b.Re^2; % [kg] equivalent mass
19
20 %% Traction evaluation
21
22 b.mux = 0.85; % friction coefficient
23 l = 2.588; % [m] wheelbase
24 h = 0.45; % [m] height of the center of mass
25 b1 = 0.45*l; % [m]
26 b2 = l - b1; % [m]
27 b.S_FWD = a.m*g*b2/l; % static part
28 b.S_RWD = a.m*g*b1/l; % static part
29 b.D = a.m*h/l; % dynamic part
30
```

Figure 60: Matlab - Vehicle.

6.1.3 Motor

Here, two motor maps are loaded, the first map collects the torque vs speed plot data, whereas the second one refers to the efficiency of the electric motor. These maps will be used in the Simulink Motor block, see 3.5.

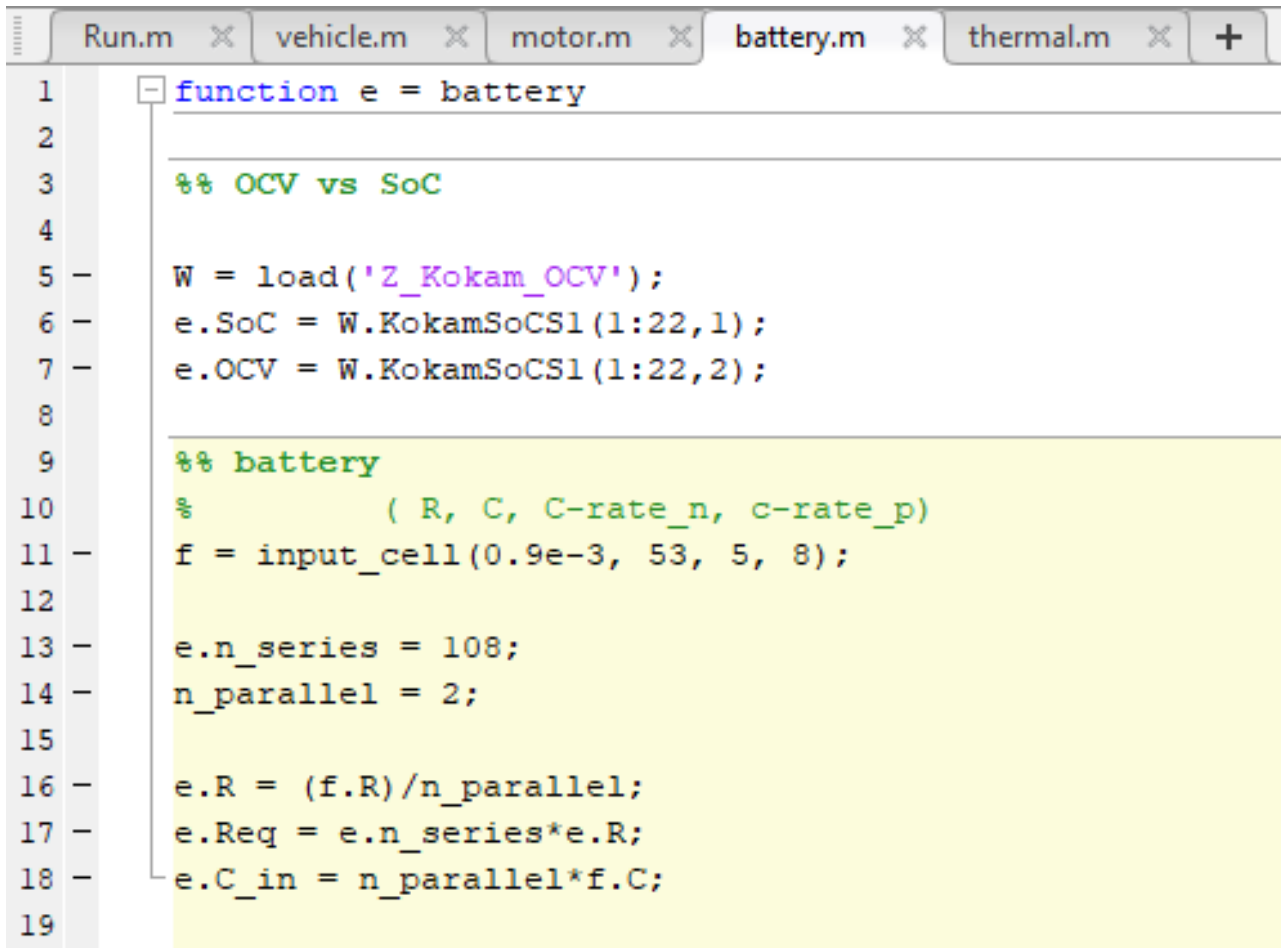


```
1 function c = motor
2
3 %% Torque map
4
5 Z = load('CS');
6 c.n = Z.MotorS1(:,1); % [rpm]
7 c.T = Z.MotorS1(:,3); % [Nm]
8
9 %% Efficiency map
10
11 E = load('CSE');
12 c.speed = E.MotorEfS1(1,2:21);
13 c.torque = flipud(E.MotorEfS1(2:41,1));
14 c.data = flipud(E.MotorEfS1(2:41, 2:21));
15
```

Figure 61: Matlab - Motor.

6.1.4 Battery

In this section is dedicated to upload the cell characteristics as the state of charge vs depth of discharge curve, internal resistance, and to evaluate battery pack parameters as total number of cells in series and in parallel. These data will be needed in the Battery Simulink block, see paragraphs 3.6.2 and 3.6.4.

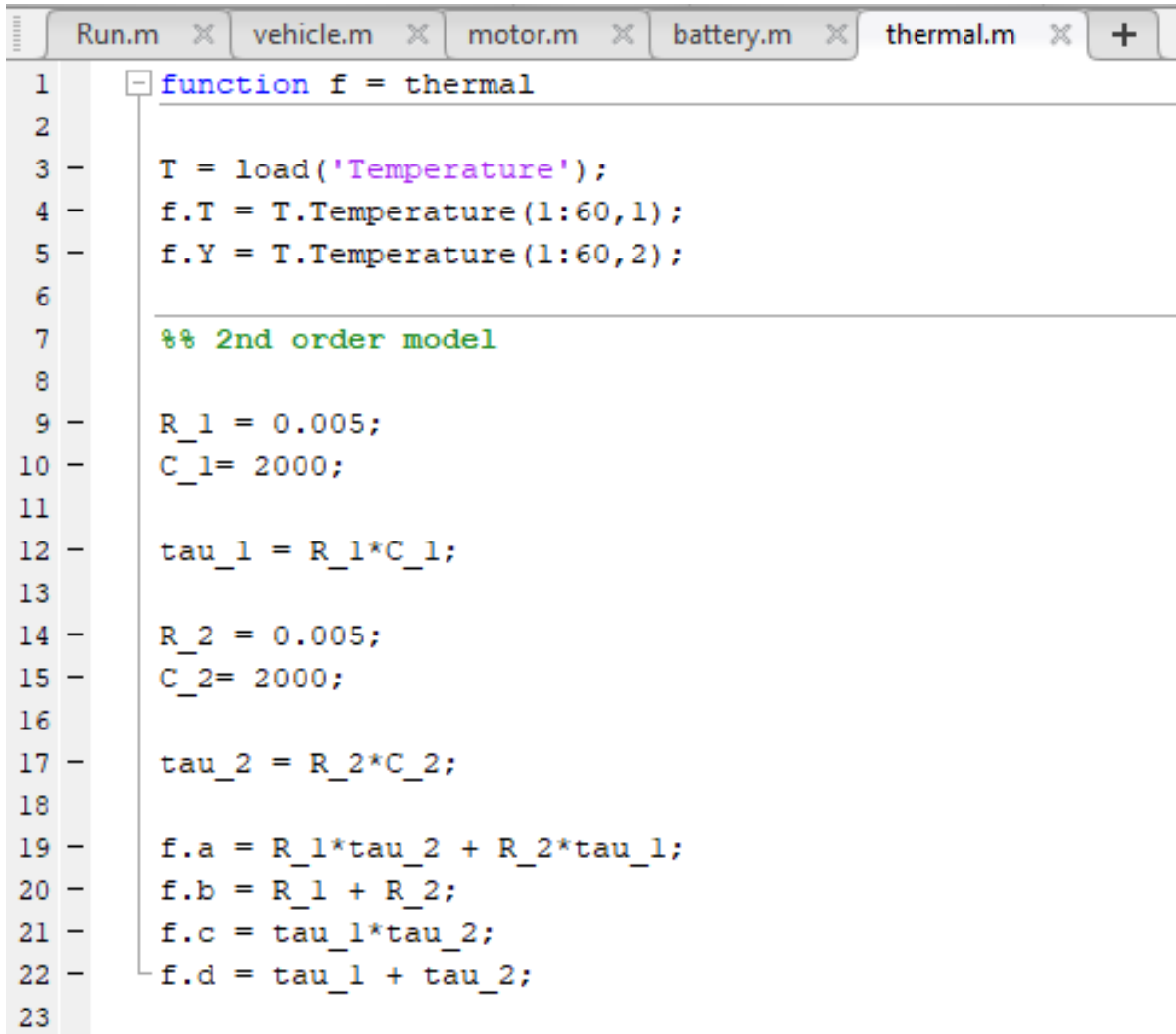
The image shows a screenshot of a MATLAB script editor window. The window title bar includes several tabs: 'Run.m', 'vehicle.m', 'motor.m', 'battery.m', and 'thermal.m'. The 'battery.m' tab is active. The script content is as follows:

```
1 function e = battery
2
3 %% OCV vs SoC
4
5 W = load('Z_Kokam_OCV');
6 e.Soc = W.KokamSoCS1(1:22,1);
7 e.OCV = W.KokamSoCS1(1:22,2);
8
9 %% battery
10 %      ( R, C, C-rate_n, c-rate_p)
11 f = input_cell(0.9e-3, 53, 5, 8);
12
13 e.n_series = 108;
14 n_parallel = 2;
15
16 e.R = (f.R)/n_parallel;
17 e.Req = e.n_series*e.R;
18 e.C_in = n_parallel*f.C;
19
```

Figure 62: Matlab - Battery.

6.1.5 Thermal model

This last section concerns the thermal battery parameters necessary to evaluate the battery pack warming. These parameters are the thermal resistance and capacitance, the Simulink block that refers to the abovementioned data is the thermal model, see 3.6.3, that is inside the battery block.



```
1 function f = thermal
2
3 T = load('Temperature');
4 f.T = T.Temperature(1:60,1);
5 f.Y = T.Temperature(1:60,2);
6
7 %% 2nd order model
8
9 R_1 = 0.005;
10 C_1= 2000;
11
12 tau_1 = R_1*C_1;
13
14 R_2 = 0.005;
15 C_2= 2000;
16
17 tau_2 = R_2*C_2;
18
19 f.a = R_1*tau_2 + R_2*tau_1;
20 f.b = R_1 + R_2;
21 f.c = tau_1*tau_2;
22 f.d = tau_1 + tau_2;
23
```

Figure 63: Matlab - Thermal model.

6.1.6 Workbench

Once the editor has been run, all the necessary data are automatically uploaded in the workbench; hence, is possible to open the Simulink file.

6.2 SIMULINK

The Simulink model allows to choose among different reference cycle and to retrieve desired output as:

- Vehicle speed
- Vehicle range
- State of Charge
- Current
- Power
- Torque
- Motor speed
- Energy consumption
- Others

Moreover, is possible to set some parameters directly from the Simulink interface, following pictures will shows how to use the Simulink tool.

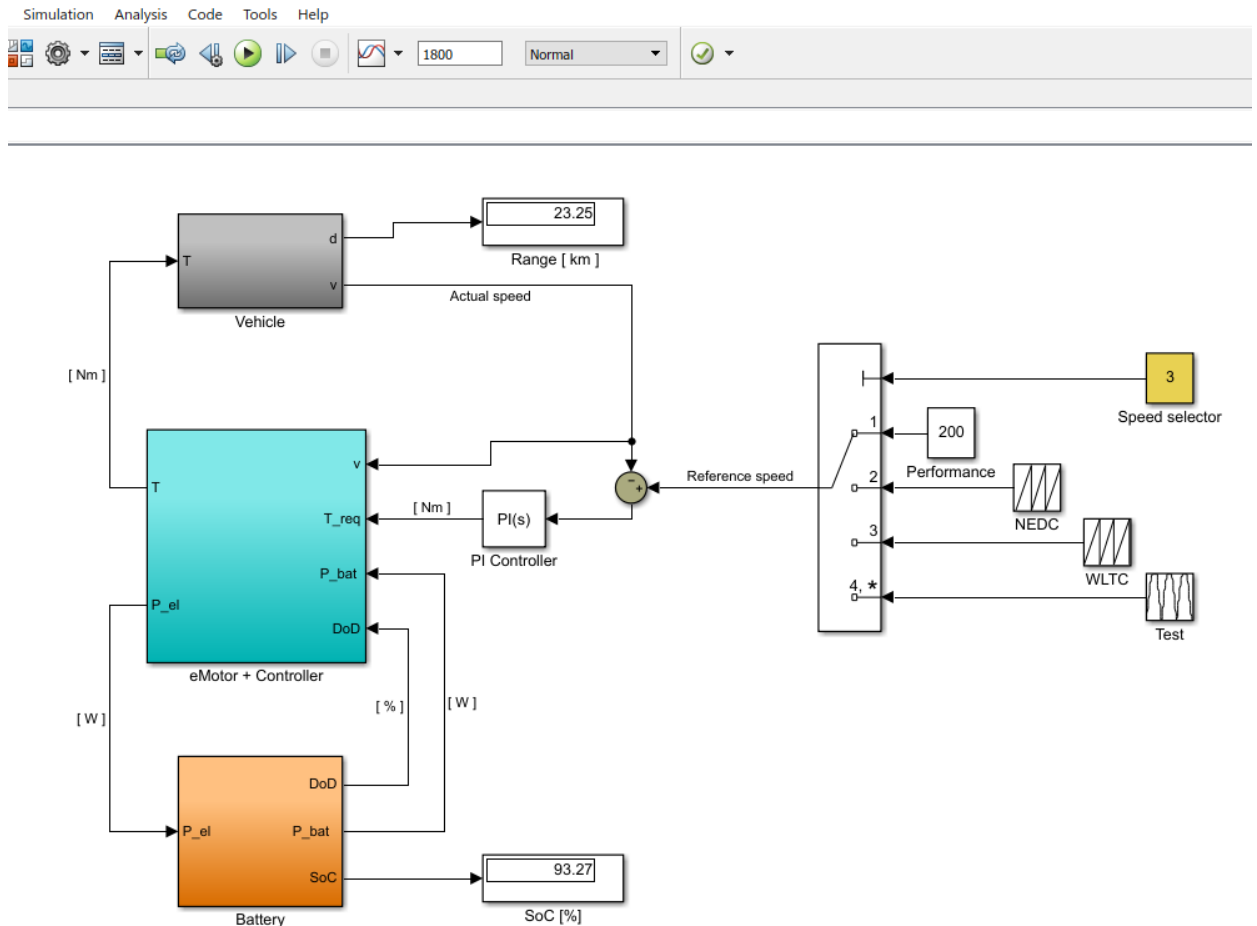


Figure 64: Simulink - Overview.

6.2.1 Speed cycles

Referring to the Figure 64: Simulink - Overview., on the right side is showed a multiport switch that can select the desired cycle:

- Performance (high gain)
- NEDC
- WLTC
- Test (see Figure 52: CS reference cycle.)

The selection is done typing the reference cycle number in the above block called button, the time for witch the cycle will be run has to be imposed on the simulation stop time display.

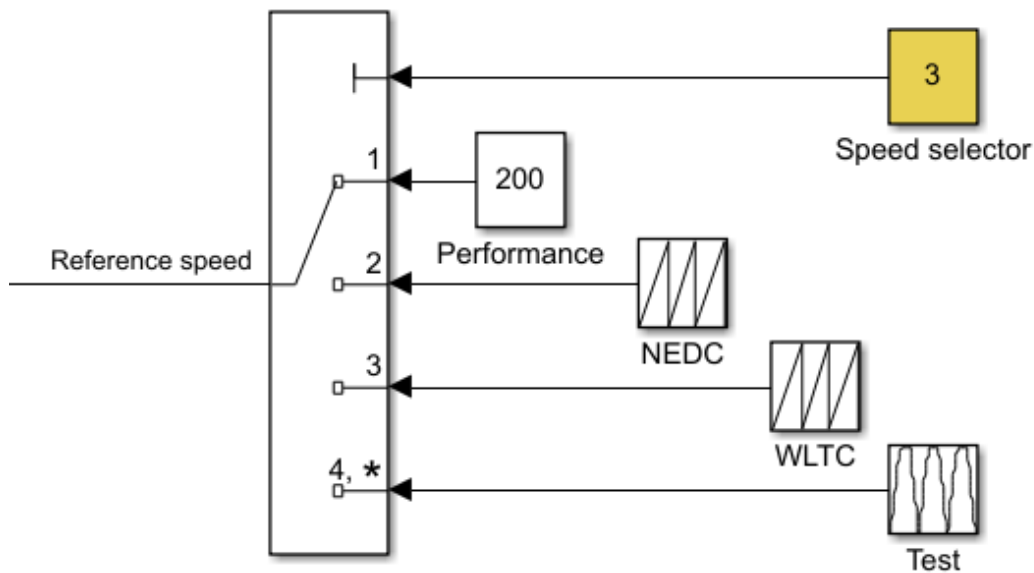


Figure 65: Simulink - Multiport switch.

7 CONCLUSION

The thesis work gives a software tool capable to simulate the longitudinal dynamic behavior, with either a forward and backward approaches, of an electric vehicle and to show the main results as vehicle performance and range.

The model subdivides the electric vehicle systems in its main components: vehicle, motor and battery, this division allows a clear vision of the relationships between each main component. The model is also equipped with the standard driving cycles needed to define the vehicle range.

A particular attention is dedicated to the battery system, which is the main core of the electric vehicle. The battery block includes the Li-ion cells characteristics and a thermal model of 2nd order, which is justified by the cells' sensitivity to high temperatures, that can compromise the battery performance and durability.

The model is available to include more specific information, when available, for instance is possible to substitute the constant internal cell resistance with a look up table, containing the resistance variation due to different operating battery pack temperature.

To conclude, the work done can be exploited to evaluate and predict the performance and range for any full electric vehicles, with an accuracy proportional with the amount of available technical data.

8 BIBLIOGRAPHY

- [1] United Nations, "United nations framework convention," 1992.
- [2] United Nations, "The Kyoto Protocol - Status of Ratification," 1999.
- [3] United Nations, "Paris Agreement," 2015.
- [4] European Commission, "A Clean Planet for all," Brussels, 2018.
- [5] European Commission, "2021 target," [Online]. Available: https://ec.europa.eu/clima/policies/transport/vehicles/cars_en.
- [6] Electrek, "Tesla (TSLA) is going to get up to \$2 billion from Fiat-Chrysler to meet emission standards," 2019. [Online]. Available: <https://electrek.co/2019/05/07/tesla-tsla-2-billion-fiat-chrysler-emission-standards/>.
- [7] European commission, [Online]. Available: https://ec.europa.eu/clima/policies/transport/vehicles/regulation_en.
- [8] iea, "Global EV Outlook 2019," May 2019. [Online]. Available: <https://www.iea.org/publications/reports/globalevoutlook2019/>.
- [9] R. D. Martino, "Modelling and simulation of the dynamic behaviour of," Université de Haute Alsace, 2005.
- [10] J. V. Porlan, "Co-simulation Methodologies for Hybrid and Electric Dynamics," 2016.
- [11] M. C. A. D. M. E. B. Aiman Nouh, "Eleves: a new software tool for electric vehicle modeling and simulation," *The World Electric Vehicle Association Journal*, vol. 1, 2007.
- [12] A. K. M. B. Bekheira Tabbache, Design and Control of the Induction Motor Propulsion of an Electric Vehicle, 2011.
- [13] D.-I. J. Merwerth, "The hybrid-synchronous machine of the new BMW i3 & i8," 2014.
- [14] M.-F. H. Thanh Anh Huynh, "Performance Analysis of Permanent Magnet Motors," *Energies*, 2018.
- [15] S. d'Ambrosio, Engine-vehicle matching, 2019.
- [16] "UNECE," [Online]. Available: <http://www.unece.org/trans/main/welcwp29.html>.
- [17] L. M. Giancarlo Genta, The Automotive Chassis, Springer, 2009.
- [18] R. N. Jazar, Vehicle Dynamics: Theory and Applications, Springer, 2008.

- [19] Cost, Effectiveness, and Deployment of Fuel Economy Technologies for Light-Duty Vehicles, Washington, D.C.: THE NATIONAL ACADEMIES PRESS, 2015.
- [20] V. Gupta, "Computation of Power of a motor in electric vehicle under traffic and dynamic conditions," 2013.
- [21] C. Amati, *Longitudinal Dynamic Project*, 2018.
- [22] J. K. A. G. G. Denis Makarchuk, "Analysis of energies and speed profiles of driving cycle for fuel consumption measurements," Riga, 2015.
- [23] CHEMTALL gmbh, "Lithium supply," 2009.
- [24] D. Rockett, "What's the Better Battery for Your Portables—Li Ion or Li Poly?," *Electronic Design*, 28 5 2018.
- [25] C. Arcus, "Tesla Model 3 & Chevy Bolt Battery Packs Examined," *Clean Technica*, 8 7 2018.
- [26] E. Loveday, "Full Details Released on 2015 Kia Soul EV's "Advanced Battery"," *INSIDEEVs*, 24 2 2014.
- [27] Kokam, "Technical specification SLPB120216216," 2019. [Online].
- [28] M. E. V. Team, "A Guide to Understanding Battery Specifications," 2008.
- [29] Tesla, [Online]. Available: https://en.wikipedia.org/wiki/Tesla_Model_S.
- [30] S. Pelloni, "Modellazione termica di batterie ad alta tensione con tecnologia Li-ion per veicoli ibridi," ALMA MATER STUDIORUM - UNIVERSITÀ DI BOLOGNA, Bologna, 2017.
- [31] A. A. A. Y. R. W. T. B. K. G. K. S. Fan He, "Reduced-order thermal modeling of liquid-cooled lithium-ion battery pack for EVs and HEVs," IEEE, 2017.
- [32] Y. X. ., S. M. I. a. Y. G. Yonghao Jia, "A Universal Scalable Thermal Resistance Model," *IEEE*, 2018.
- [33] BRUSA, "Drive section," [Online]. Available: <https://www.brusa.biz/en.html>.
- [34] T. F. I. M. M. V. J. M. V. M. Naveen Kumar Arora, *Environmental sustainability: challenges and viable solutions*, Springer, 2018.